

# ENGINEERING OF BIOMATERIALS

INŻYNIERIA BIOMATERIAŁÓW

JOURNAL OF POLISH SOCIETY FOR BIOMATERIALS AND FACULTY OF MATERIALS SCIENCE AND CERAMICS AGH-UST

CZASOPISMO POLSKIEGO STOWARZYSZENIA BIOMATERIAŁÓW I WYDZIAŁU INŻYNIERII MATERIAŁOWEJ I CERAMIKI AGH

**Number 140**

Numer 140

**Volume XX**

Rok XX

**APRIL 2017**

KWIECIEŃ 2017

**ISSN 1429-7248**

**PUBLISHER:**

WYDAWCA:

**Polish Society  
for Biomaterials  
in Krakow**

Polskie  
Stowarzyszenie  
Biomateriałów  
w Krakowie

**EDITORIAL**

**COMMITTEE:**

KOMITET

REDAKCYJNY:

**Editor-in-Chief**

Redaktor naczelny

**Jan Chłopek**

**Editor**

Redaktor

**Elżbieta Pamuła**

**Secretary of editorial**

Sekretarz redakcji

**Design**

Projekt

**Katarzyna Trała**

**Augustyn Powroźnik**

**ADDRESS OF**

**EDITORIAL OFFICE:**

ADRES REDAKCJI:

**AGH-UST**

**30/A3, Mickiewicz Av.**

**30-059 Krakow, Poland**

Akademia

Górnictwo-Hutnicza

al. Mickiewicza 30/A-3

30-059 Kraków

**Issue: 250 copies**

Nakład: 250 egz.

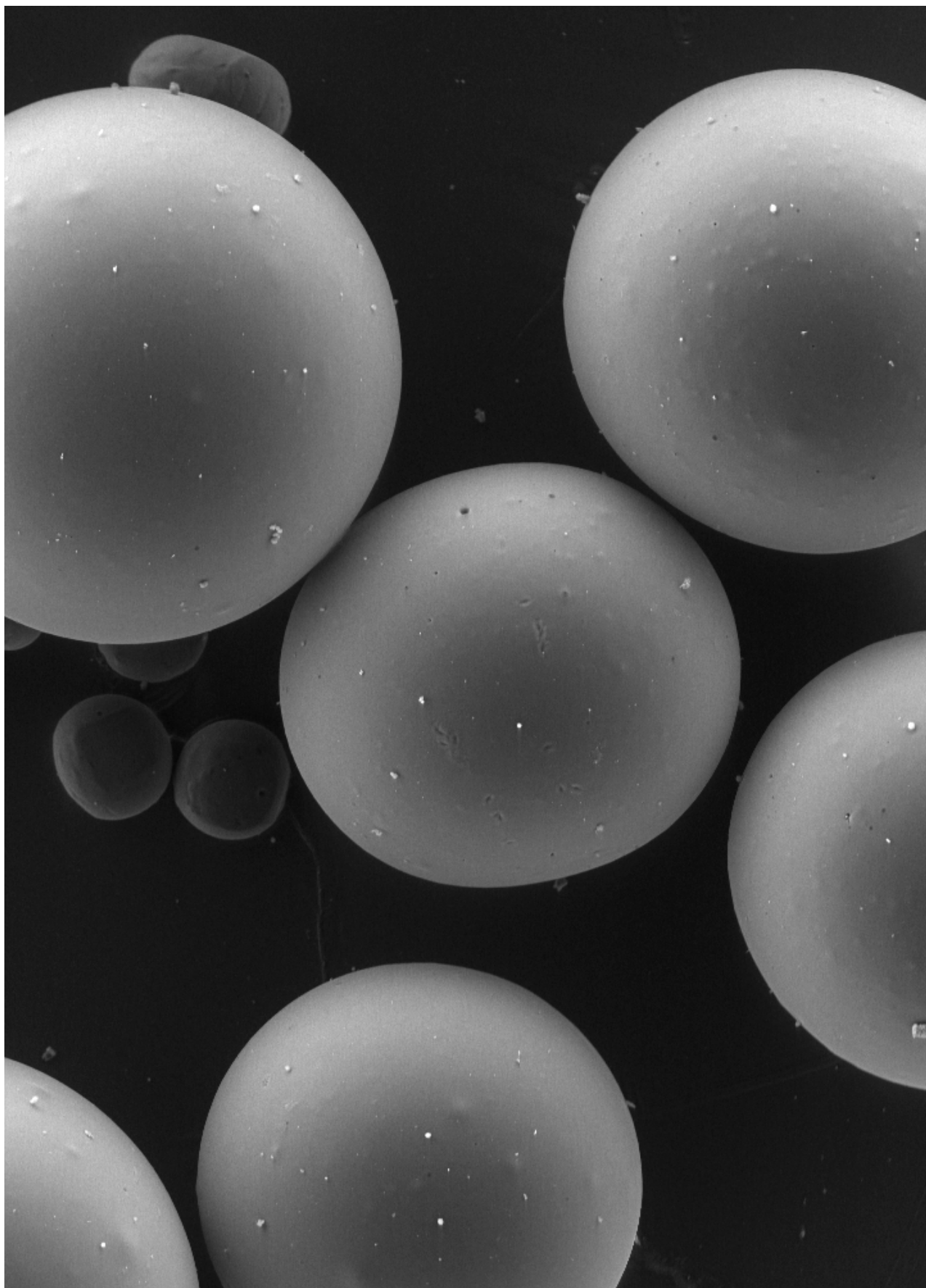
**Scientific Publishing**

**House AKAPIT**

Wydawnictwo Naukowe

AKAPIT

e-mail: [wn@akapit.krakow.pl](mailto:wn@akapit.krakow.pl)



**EDITORIAL BOARD  
KOMITET REDAKCYJNY**

**EDITOR-IN-CHIEF**

Jan Chłopek - AGH UNIVERSITY OF SCIENCE AND TECHNOLOGY, KRAKOW, POLAND

**EDITOR**

Elżbieta Pamuła - AGH UNIVERSITY OF SCIENCE AND TECHNOLOGY, KRAKOW, POLAND

**INTERNATIONAL EDITORIAL BOARD  
MIĘDZYNARODOWY KOMITET REDAKCYJNY**

Iulian Antoniac - UNIVERSITY POLITEHNICA OF BUCHAREST, ROMANIA

Lucie Bacakova - ACADEMY OF SCIENCE OF THE CZECH REPUBLIC, PRAGUE, CZECH REPUBLIC

Romuald Będziński - UNIVERSITY OF ZIELONA GÓRA, POLAND

Marta Błażewicz - AGH UNIVERSITY OF SCIENCE AND TECHNOLOGY, KRAKOW, POLAND

Stanisław Błażewicz - AGH UNIVERSITY OF SCIENCE AND TECHNOLOGY, KRAKOW, POLAND

Maria Borczuch-Łączka - AGH UNIVERSITY OF SCIENCE AND TECHNOLOGY, KRAKOW, POLAND

Wojciech Chrzanowski - UNIVERSITY OF SYDNEY, AUSTRALIA

Jan Ryszard Dąbrowski - BIAŁYSTOK TECHNICAL UNIVERSITY, POLAND

Timothy Douglas - UNIVERSITY OF GENT, BELGIUM

Christine Dupont-Gillain - UNIVERSITÉ CATHOLIQUE DE LOUVAIN, BELGIUM

Matthias Epple - UNIVERSITY OF DUISBURG-ESSEN, GERMANY

Robert Hurt - BROWN UNIVERSITY, PROVIDENCE, USA

James Kirkpatrick - JOHANNES GUTENBERG UNIVERSITY, MAINZ, GERMANY

Ireneusz Kotela - CENTRAL CLINICAL HOSPITAL OF THE MINISTRY OF THE INTERIOR AND ADMINISTR. IN WARSAW, POLAND

Małgorzata Lewandowska-Szumieł - MEDICAL UNIVERSITY OF WARSAW, POLAND

Jan Marciniak - SILESIAN UNIVERSITY OF TECHNOLOGY, ZABRZE, POLAND

Ion N. Mihailescu - NATIONAL INSTITUTE FOR LASER, PLASMA AND RADIATION PHYSICS, BUCHAREST, ROMANIA

Sergey Mikhailovsky - UNIVERSITY OF BRIGHTON, UNITED KINGDOM

Stanisław Mitura - KOSZALIN UNIVERSITY OF TECHNOLOGY, POLAND

Piotr Niedzielski - TECHNICAL UNIVERSITY OF LODZ, POLAND

Abhay Pandit - NATIONAL UNIVERSITY OF IRELAND, GALWAY, IRELAND

Stanisław Pielka - WROCLAW MEDICAL UNIVERSITY, POLAND

Vehid Salih - UCL EASTMAN DENTAL INSTITUTE, LONDON, UNITED KINGDOM

Jacek Składzień - JAGIELLONIAN UNIVERSITY, COLLEGIUM MEDICUM, KRAKOW, POLAND

Andrei V. Stanishevsky - UNIVERSITY OF ALABAMA AT BIRMINGHAM, USA

Anna Ślósarczyk - AGH UNIVERSITY OF SCIENCE AND TECHNOLOGY, KRAKOW, POLAND

Tadeusz Trzaska - UNIVERSITY SCHOOL OF PHYSICAL EDUCATION, POZNAŃ, POLAND

Dimitris Tsipas - ARISTOTLE UNIVERSITY OF THESSALONIKI, GREECE

## Wskazówki dla autorów

1. Prace do opublikowania w kwartalniku „Engineering of Biomaterials / Inżynieria Biomateriałów” przyjmowane będą wyłącznie z tłumaczeniem na język angielski. Obcokrajowców obowiązuje tylko język angielski.
2. Wszystkie nadsyłane artykuły są recenzowane.
3. Materiały do druku prosimy przysyłać na adres e-mail: kabe@agh.edu.pl.
4. Struktura artykułu:
  - TYTUŁ • Autorzy i instytucje • Streszczenie (200-250 słów) • Słowa kluczowe (4-6) • Wprowadzenie • Materiały i metody • Wyniki i dyskusja • Wnioski • Podziękowania • Piśmiennictwo
5. Autorzy przesyłają pełną wersję artykułu, łącznie z ilustracjami, tabelami, podpisami i literaturą w jednym pliku. Ilustracje, tabele, podpisy i literatura powinny być umieszczone również w wersji angielskiej. Artykuł w tej formie przesyłany jest do recenzentów. Dodatkowo autorzy proszeni są o przesłanie materiałów ilustracyjnych (rysunki, schematy, fotografie, wykresy) w oddzielnych plikach (format np. .jpg, .gif, .tiff, .bmp). Rozdzielczość rysunków min. 300 dpi. Wszystkie rysunki i wykresy powinny być czarno-białe lub w odcieniach szarości i ponumerowane cyframi arabskimi. W tekście należy umieścić odnośniki do rysunków i tabel. W tabelach i na wykresach należy umieścić opisy polskie i angielskie.
6. Na końcu artykułu należy podać wykaz piśmiennictwa w kolejności cytowania w tekście i kolejno ponumerowany.
7. Redakcja zastrzega sobie prawo wprowadzenia do opracowań autorskich zmian terminologicznych, poprawek redakcyjnych, stylistycznych, w celu dostosowania artykułu do norm przyjętych w naszym czasopiśmie. Zmiany i uzupełnienia merytoryczne będą dokonywane w uzgodnieniu z autorem.
8. Opinia lub uwagi recenzentów będą przekazywane Autorowi do ustosunkowania się. Nie dostarczenie poprawionego artykułu w terminie oznacza rezygnację Autora z publikacji pracy w naszym czasopiśmie.
9. Za publikację artykułów redakcja nie płaci honorarium autorskiego.
10. Adres redakcji:
  - Czasopismo
  - „Engineering of Biomaterials / Inżynieria Biomateriałów”
  - Akademia Górniczo-Hutnicza im. St. Staszica
  - Wydział Inżynierii Materiałowej i Ceramiki
  - al. Mickiewicza 30/A-3, 30-059 Kraków
  - tel. (48) 12 617 25 03, 12 617 25 61
  - tel./fax: (48) 12 617 45 41
  - e-mail: chlopek@agh.edu.pl, kabe@agh.edu.pl

Szczegółowe informacje dotyczące przygotowania manuskryptu oraz procedury recenzowania dostępne są na stronie internetowej czasopisma:  
[www.biomat.krakow.pl](http://www.biomat.krakow.pl)

## Warunki prenumeraty

Zamówienie na prenumeratę prosimy przysyłać na adres: apowroz@agh.edu.pl, tel/fax: (48) 12 617 45 41  
Cena pojedynczego numeru wynosi 20 PLN  
Konto:  
Polskie Stowarzyszenie Biomateriałów  
30-059 Kraków, al. Mickiewicza 30/A-3  
ING Bank Śląski S.A. O/Kraków  
nr rachunku 63 1050 1445 1000 0012 0085 6001

Prenumerata obejmuje 4 numery regularne i nie obejmuje numeru specjalnego (materiały konferencyjne).

## Instructions for authors

1. Papers for publication in quarterly journal „Engineering of Biomaterials / Inżynieria Biomateriałów” should be written in English.
2. All articles are reviewed.
3. Manuscripts should be submitted to editorial office by e-mail to kabe@agh.edu.pl.
4. A manuscript should be organized in the following order:
  - TITLE • Authors and affiliations • Abstract (200-250 words) • Keywords (4-6) • Introduction • Materials and Methods • Results and Discussions • Conclusions • Acknowledgements • References
5. All illustrations, figures, tables, graphs etc. preferably in black and white or grey scale should be additionally sent as separate electronic files (format .jpg, .gif, .tiff, .bmp). High-resolution figures are required for publication, at least 300 dpi. All figures must be numbered in the order in which they appear in the paper and captioned below. They should be referenced in the text. The captions of all figures should be submitted on a separate sheet.
6. References should be listed at the end of the article. Number the references consecutively in the order in which they are first mentioned in the text.
7. The Editors reserve the right to improve manuscripts on grammar and style and to modify the manuscripts to fit in with the style of the journal. If extensive alterations are required, the manuscript will be returned to the authors for revision.
8. Opinion or notes of reviewers will be transferred to the author. If the corrected article will not be supplied on time, it means that the author has resigned from publication of work in our journal.
9. Editorial does not pay author honorarium for publication of article.
10. Address of editorial office:
  - Journal
  - „Engineering of Biomaterials / Inżynieria Biomateriałów”
  - AGH University of Science and Technology
  - Faculty of Materials Science and Ceramics
  - 30/A-3, Mickiewicz Av., 30-059 Krakow, Poland
  - tel. (48) 12) 617 25 03, 12 617 25 61
  - tel./fax: (48) 12 617 45 41
  - e-mail: chlopek@agh.edu.pl, kabe@agh.edu.pl

Detailed information concerning manuscript preparation and review process are available at the journal's website:  
[www.biomat.krakow.pl](http://www.biomat.krakow.pl)

## Subscription terms

Subscription rates:  
Cost of one number: 20 PLN  
Payment should be made to:  
Polish Society for Biomaterials  
30/A3, Mickiewicz Av.  
30-059 Krakow, Poland  
ING Bank Śląski S.A.  
account no. 63 1050 1445 1000 0012 0085 6001

Subscription includes 4 issues and does not include special issue (conference materials).

Join the ISBPPB 2018 Conference to hear the latest research findings on polymers in medicine and enjoy many opportunities to network with colleagues and new friends from all over the world

# 4th International Conference on Biomedical Polymers & Polymeric Biomaterials

15–18 July 2018, Kraków, POLAND



## ISBPPB 2018 topics:

biodegradable polymers, hydrogels, polysilanes, polysaccharides, polyurethanes, polymer foams, smart polymers, shape memory polymers, polymers for dental and orthopedic applications, blood-contacting polymers, polymers for skin grafting, polymers for targeted drug delivery, polymers for tissue engineering, **and many more**

## ISBPPB 2018 program:

- Plenary/Invited Lectures
- Oral Presentations
- Young Researcher Presentations
- Poster Session
- Exhibitions

[www.isbppb2018.org](http://www.isbppb2018.org)

## SPIS TREŚCI CONTENTS

**STRUCTURE AND MORPHOLOGY OF WHITLOCKITE  
 COATING ELECTROPHORETICALLY DEPOSITED  
 ON NiTi SHAPE MEMORY ALLOY**  
 KAROLINA DUDEK, TOMASZ GORYCZKA **2**

**MODIFICATION OF PLGA MICROSPHERES' MICRO-  
 STRUCTURE FOR APPLICATION AS CELL CARRIERS  
 IN MODULAR TISSUE ENGINEERING**  
 BARTOSZ MIELAN, MAŁGORZATA KROK-BORKOWICZ,  
 KINGA PIELICHOWSKA, ELŻBIETA PAMUŁA **7**

**DETONATION NANODIAMOND PARTICLES MODIFIED  
 BY NON-STEROIDAL ANTI-INFLAMMATORY  
 DRUGS *IN VITRO* EXAMINATION**  
 KATARZYNA MITURA, PIOTR WILCZEK, ALEKSANDRA  
 NIEMIEC-CYGANEK, MAŁGORZATA MORENC,  
 MARIUSZ DUDEK, ANNA SOB CZYK-GUZENDA,  
 JUSTYNA FRACZYK, BEATA KOLESIŃSKA **12**

**INTERACTIONS OF CARBON NANOPARTICLES  
 FROM PACKAGINGS WITH COMPONENTS  
 OF FOOD, DRUGS AND BIOLOGICALLY  
 ACTIVE MOLECULES - A REVIEW**  
 JOLANTA WRÓBLEWSKA-KREPSZTUŁ, IWONA  
 MICHALSKA-POŻOGA, MIECZYŚLAW SZCZYPIŃSKI,  
 PIOTR WILCZEK, TOMASZ RYDZKOWSKI **21**



WERSJA PAPIEROWA CZASOPISMA „ENGINEERING OF BIOMATERIALS / INŻYNIERIA BIOMATERIAŁÓW” JEST JEGO WERSJĄ PIERWOTNĄ  
 PRINTED VERSION OF „ENGINEERING OF BIOMATERIALS / INŻYNIERIA BIOMATERIAŁÓW” IS A PRIMARY VERSION OF THE JOURNAL



# STRUCTURE AND MORPHOLOGY OF WHITLOCKITE COATING ELECTROPHORETICALLY DEPOSITED ON NiTi SHAPE MEMORY ALLOY

KAROLINA DUDEK\*, TOMASZ GORYCZKA

UNIVERSITY OF SILESIA, INSTITUTE OF MATERIALS SCIENCE,  
75 PULKU PIECHOTY 1A, 41-500 CHORZOW, POLAND

\* E-MAIL: K.DUDEK@ICIMB.PL

## Abstract

*In order to improve the biocompatibility of NiTi shape memory alloy, the surface was modified by formation of multifunctional layer consisted of titanium oxides and whitlockite ceramic. Amorphous TiO<sub>2</sub> inter-layer was produced on NiTi substrate by autoclaving at 134°C for 30 minutes while the following whitlockite coatings were deposited using electrophoresis (EPD). Electrophoresis was performed under different voltage (from 20 to 80 V) at time periods (from 30 to 120 s). Applied deposition parameters 20 V and 60 s resulted in forming homogenous whitlockite coating, consisted of  $\beta$ -Ca<sub>3</sub>(PO<sub>4</sub>)<sub>2</sub> and  $\beta$ -Ca<sub>2</sub>P<sub>2</sub>O<sub>7</sub>, on passivated NiTi alloy. In the next step, the material was heat-treated in vacuum condition at 1000°C for 2 h. As a result of sintering crystallization of titanium oxides was observed. The obtained layer was cracks-free. Applied deposition process increased the roughness of surface. Deposited whitlockite agglomerates had an average thickness ca. 5.6  $\mu$ m. The structure of CaP coating material after applied heat-treatment remained unchanged in comparison to initial powder material. However, the partial decomposition of NiTi parent phase to equilibrium ones was observed. The whitlockite coating was also observed to have no impact on the martensitic transformation responsible for shape memory effect. Additionally, applied sintering condition changed the sequence of martensitic transformation from one to two-step.*

**Keywords:**  $\beta$ -TCP (whitlockite), electrophoretic deposition (EPD), NiTi shape memory alloy (SMA), surface modification

[*Engineering of Biomaterials* 140 (2017) 2-6]

## Introduction

The NiTi shape memory alloys (SMA) with its chemical composition near to that of equiatomic ones are used in a wide range of biomedical fields. They are widely applied in orthodontics, soft tissue surgery, cardiovascular applications and in orthopaedic. However, their biomechanical properties make it more suitable for bone fixation than other metallic materials [1,2]. Nevertheless, the applications of the NiTi shape memory alloy as long-term implants can be limited by the possibility of toxic nickel ions migration into the organism due to corrosion. In order to improve its corrosion resistance and form the diffusion barrier for potentially released Ni ions, the surface of NiTi alloys can be modified by formation of multifunctional layers [3-5]. The surface of NiTi is covered with layers based on diamond-like phases, titanium oxides, titanium carbides and nitrides, polymers,

apatites or composites [3-7]. It is desirable that the protective layers increase the functionality of the implant surface, for example by enhancing the osseointegration. The best bonding of the metal implant surface to bone tissue is achieved by producing calcium phosphate-based (CaPs) coatings such as hydroxyapatite (HAp) or whitlockite ceramic (TCP) [8]. Calcium phosphate ceramics (CaPs) are promising materials for medical applications. The interest in these materials is clear due to their high chemical similarity to the inorganic parts of bones and teeth of mammals. Calcium phosphates are bioactive and conduct bone apposition by direct bone bonding [9-11].

In the case of the NiTi alloy, it is very important to choose a low-temperature technique of surface modification as possible. High temperature treatment can lead to decomposition of the B2 phase and thereby may affect the shape memory effects. Electrophoretic deposition (EPD) is one of the techniques applied for surface modification, which can be carried out at ambient temperature. Moreover, the EPD is reproducible, inexpensive and rapid. These techniques additionally enable controlling the coating thickness, its uniformity and deposition rate by alteration of deposition parameters such as voltage and time [12,13].

The main aim of presented results was focused on the biocompatibility intensification of NiTi SMA done by its surface modification. The technology of material preparation was focused on the passivation of NiTi substrate by autoclaving and following electrophoretic deposition (EPD) of whitlockite ceramic ( $\beta$ -TCP).

## Materials and Methods

A commercially available NiTi alloy, with the following chemical composition of 50.6 at.% Ni and 49.4 at.% Ti (Memry GmbH), was used as substrate for layers deposition. Before EPD, the substrate was passivated in autoclave at 134°C for 30 min. The autoclaving resulted in formation of a thin amorphous TiO<sub>2</sub> layer [14] what improves the corrosion resistance [6]. Moreover, forming the oxide titanium interlayer on titanium alloys results in increased adhesion of following deposited CaPs coatings [15].

The commercially available powder of whitlockite (nGimat), consisted of 87.1  $\pm$  1.0 wt.%  $\beta$ -Ca<sub>3</sub>(PO<sub>4</sub>)<sub>2</sub> ( $\beta$ -TCP) and 12.9  $\pm$  0.2 wt.%  $\beta$ -Ca<sub>2</sub>P<sub>2</sub>O<sub>7</sub>, was used to prepare a colloidal suspension having a concentration of 0.1 wt.% the powder in 99.9% ethanol (Avantor). The powder was crystalline and the particles had an irregular shape. The mixture was put into a magnetic stirrer (30 min) and then transferred to an ultrasonic bath (30 min). The average size of the ceramic particles in the colloidal suspension was ca. 550 nm. Zeta potential and conductivity of suspension at pH 6.7 were found to be 33.5  $\pm$  0.3 mV and 0.61  $\mu$ S/cm, respectively [16].

Afterwards, electrophoretic deposition (EPD) under cathodic condition and at room temperature was performed to cover the passivated NiTi substrate by CaPs particles. The constant voltages (from 20 to 80 V) at time periods (from 30 to 120 s) were applied. After deposition, the green form coatings were dried for 24 h at ambient temperature. Then, in order to consolidate and increase the adhesion strength of the ceramic coating to the metal substrate samples were heat treated in vacuum furnace at 1000°C for 2 h.

Phase identification was carried out using an X-ray diffraction pattern (XRD) measured with an X'PertPro diffractometer with monochromatized Cu K $\alpha$  radiation. The coated NiTi alloy was examined by the grazing incidence X-ray diffraction technique (GIXD). The GIXRD patterns were collected at constant incidence angles of 0.2° at room temperature.

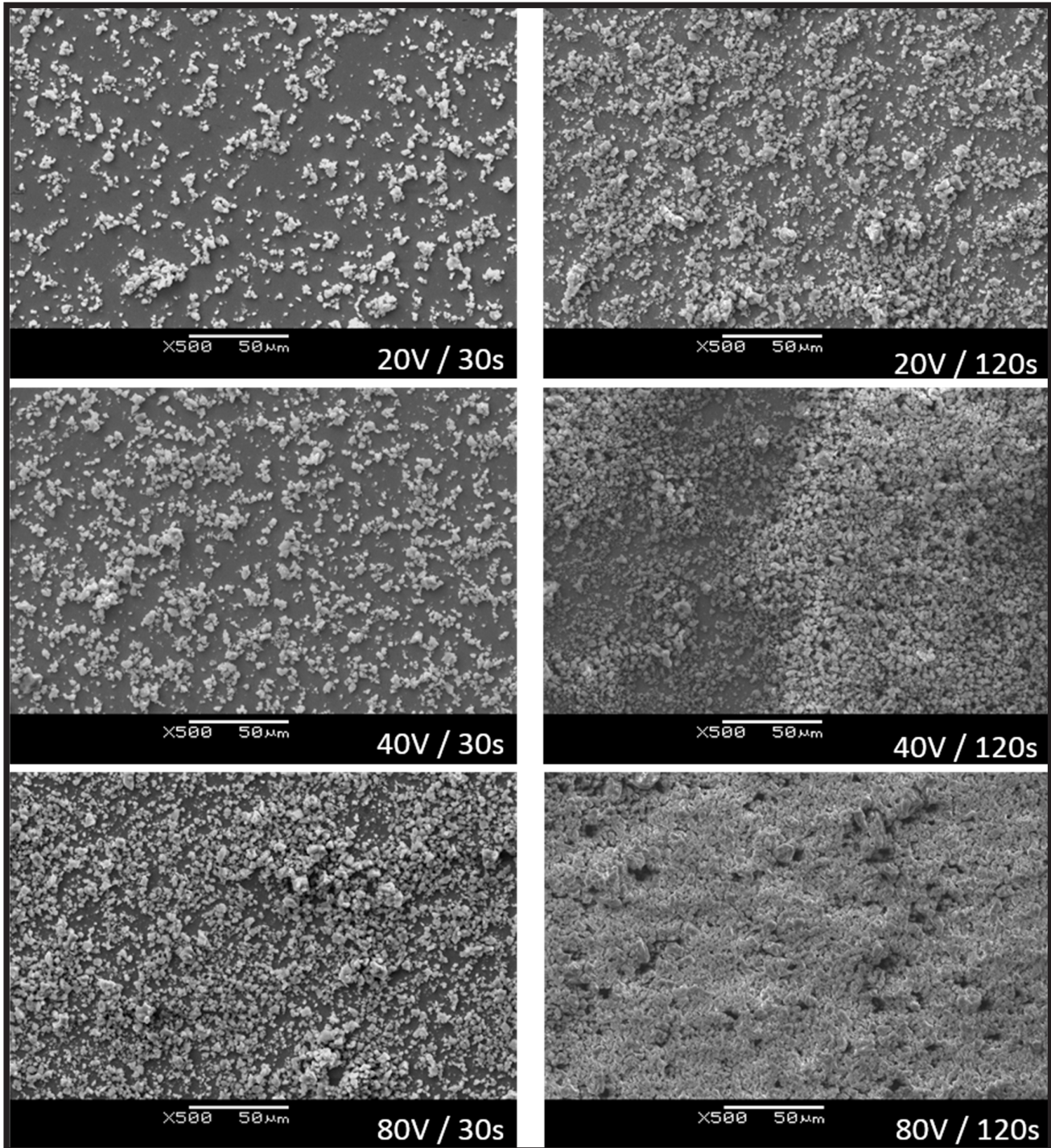
The morphology of deposited coatings was observed using a JEOL JSM-6480 scanning electron microscope (SEM) coupled with an Energy Dispersive Spectrometer (EDS).

The surface features of coatings, deposited under different parameters and after heat treatment, like Ra (arithmetic mean surface roughness), Rz (surface roughness depth) and Rt (total height of the roughness profile) were measured in line mode using a Mitutoyo SurfTest SJ-500 profilometer at 100 Hz sampling frequency and 20 mm/s scanning rate.

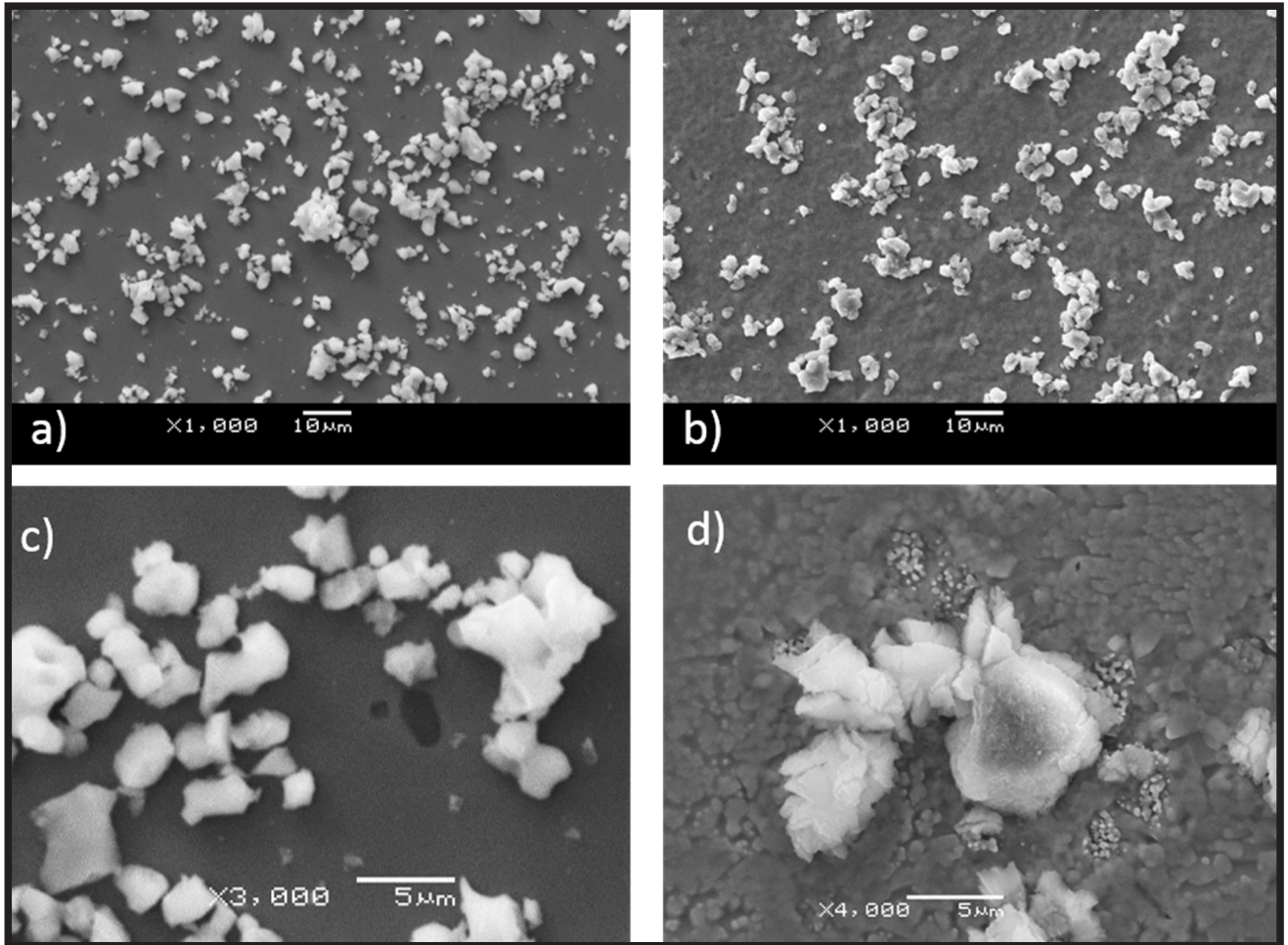
Differential scanning calorimetry (DSC) was used to study the influence of the deposition process on the course of martensitic transformation. Measurements were taken before and after sintering, using a DSC1 Mettler Toledo calorimeter. The heating/cooling rate of 10°C per minute was applied.

## Results and Discussions

The previously done studies revealed that applied voltage and deposition time have a great impact on the quality of CaPs coatings electrophoretically deposited on the passivated NiTi substrate [16,17]. Due to lower voltage and deposition time, the whitlockite ceramics particles spread on the surface heterogeneously forming larger agglomerates (FIG. 1). It was found that between agglomerates a relatively thin film consisting of calcium, phosphorus and oxygen forming phosphate groups was created [16]. Increase in the quantity of deposited particles, at the constant voltage with elongation deposition time, in comparison to constant time and increase in voltage was observed. Deposition parameters (80 V/120 s) impact on increase in density and thickness of the coating (FIG. 1).



RYS. 1. Obrazy SEM stopu NiTi pokrytego warstwami w różnych warunkach.  
FIG. 1. SEM images of NiTi coated substrate at different conditions.



RYS. 2. Obrazy SEM stopu NiTi po osadzeniu warstw w 20 V przez 60 s (a, c) oraz po obróbce cieplnej w 1000°C przez 2 godz. (b, d).

FIG. 2. SEM images of NiTi coated substrate after deposition at 20 V for 60 s (a, c) and after following heat treatment at 1000°C for 2 h (b, d).

TABELA 1. Parametry chropowatości pasywowanego stopu NiTi oraz po osadzeniu i obróbce cieplnej.  
TABLE 1. Roughness parameters of passivated and coated NiTi surface before and after sintering.

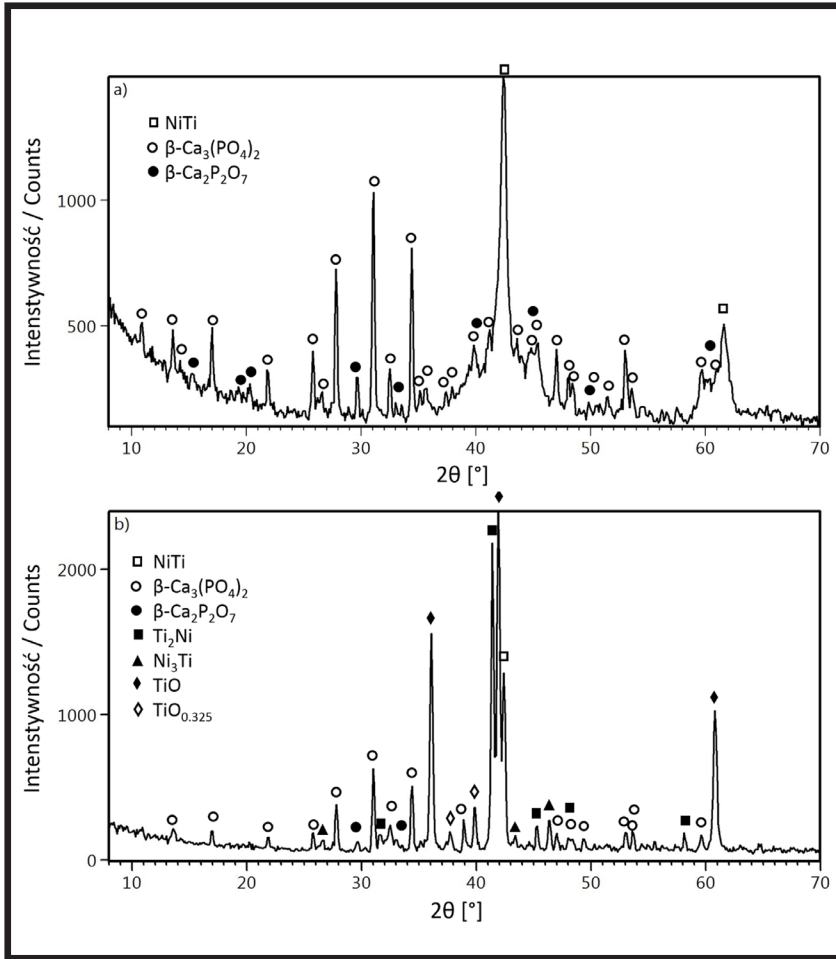
	Ra [ $\mu\text{m}$ ]	Rz [ $\mu\text{m}$ ]	Rt [ $\mu\text{m}$ ]
Pasywowany stop NiTi / Passivated NiTi alloy	0.04(1)	0.2(1)	0.3(1)
Powłoka TCP (20 V / 60 s) po spiekaniu (1000°C / 2 h) TCP coating (20 V / 60 s) after sintering (1000°C / 2 h)	0.59(7)	4.2(3)	5.6(4)

The applied heat treatment conditions (1000°C for 2 h) resulted in a visible change in the morphology of the coating (FIG. 2). The areas between the agglomerates changed from smooth to rough. It may be caused by the intensification of the titanium oxide crystallization from the amorphous oxide layer, previously formed on NiTi substrate during the autoclaving. Changes in the roughness of these areas may also be due to the considerable dispersion of powdered particles in the suspension, which also resulted in uneven grain growth after the sintering process. Moreover, the presence of crystallized clusters of fine particles, especially close to CaP aggregates, was also stated (FIG. 2d).

The profilometry results presented in TABLE 1 showed that deposition process of whitlockite ceramics increased the roughness of the surface. The value of average roughness (Ra), surface roughness depth (Rz) and total height of the roughness profile (Rt) increased compared to the passivated NiTi surface. The uneven and rough surface improves the adhesion of cells and tissues to the coating surface and

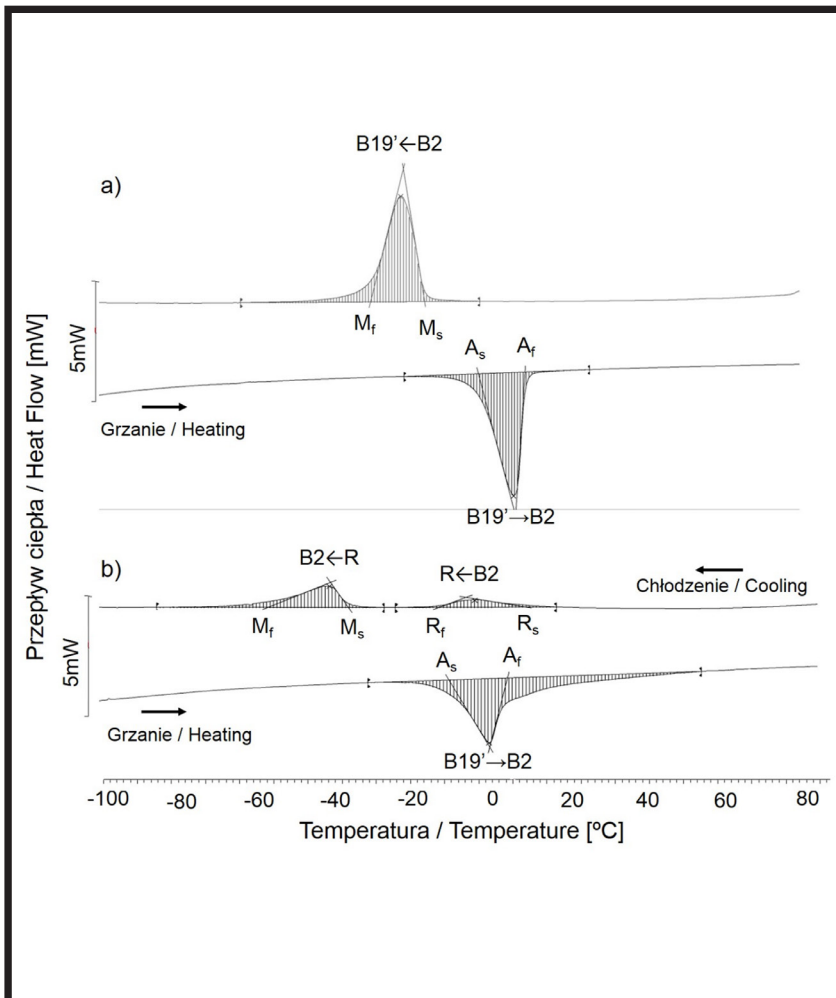
promotes a shorter healing process than the smoother one [18]. The value of Rt parameter indicates also an average agglomerate thickness of about 5.6  $\mu\text{m}$ .

Diffraction data (GIXRD) collected for samples after deposition and after sintering process (FIG. 3a, b) revealed well-defined peaks both of  $\beta$ -TCP (ICDD - PDF 04-008-8714) with rhombohedral structure (R-3c) and trace amount of  $\beta$ - $\text{Ca}_2\text{P}_2\text{O}_7$  phase with tetragonal structure (P4<sub>1</sub>) (ICDD-PDF 04-009-8733). The presence of diffraction lines from whitlockite decomposition products was not proved. The applied heat treatment (1000°C/2 h in vacuum) resulted in a partial decomposition of NiTi substrate (ICDD - PDF 01-078-4618) to equilibrium phases:  $\text{Ti}_2\text{Ni}$  (ICDD - PDF 04-007-1531) with cubic structure (Fd-3m) and  $\text{Ni}_3\text{Ti}$  with hexagonal structure (P6<sub>3</sub>/mmc). In addition, the appearance of diffraction lines belonging to non-stoichiometric  $\text{TiO}_{0.325}$  with hexagonal structure (P6<sub>3</sub>/mmc) (ICDD - PDF 04-005-4356) and TiO with cubic structure (Fm-3m) (ICDD - PDF 04-016-4319) were identified.



RYS. 3. Dyfraktogram rentgenowski zmierzony przy stałym kącie padania wiązki pierwotnej ( $0,2^\circ$ ) dla powłoki osadzonej przy 20 V w czasie 60 s (a) oraz po obróbce cieplnej w  $1000^\circ\text{C}$  przez 2 godz. (b).

FIG. 3. The GIXRD patterns measured at incidence angle of  $0.2^\circ$  for coating deposited at 20 V for 60 s (a) and after heat treatment at  $1000^\circ\text{C}$  for 2 h (b).



RYS. 4. Krzywe DSC dla wyjściowego stopu NiTi (a) oraz po osadzeniu warstw TCP i spiekaniu  $1000^\circ\text{C}$  przez 2 godz. (b), gdzie:  $A_s$  - temperatura początku odwrotnej przemiany martenzytycznej,  $A_f$  - temperatura końca odwrotnej przemiany martenzytycznej,  $M_s$  - temperatura początku przemiany martenzytycznej,  $M_f$  - temperatura końca przemiany martenzytycznej,  $R_s$  - temperatura początku przemiany B2→R,  $R_f$  - temperatura końca przemiany B2→R, B2→R→B19' - przemiana martenzytyczna, B19'→B2 - odwrotna przemiana martenzytyczna.

FIG. 4. DSC cooling/heating curves measured for an initial NiTi substrate (a) and after deposition of TCP and sintering at  $1000^\circ\text{C}$  for 2 h (b), where:  $A_s$  - start temperature of the reverse martensitic transformation,  $A_f$  - finish temperature of the reverse martensitic transformation,  $M_s$  - start temperature of the forward martensitic transformation,  $M_f$  - finish temperature of the forward martensitic transformation,  $R_s$  - start temperature of the B2→R transition,  $R_f$  - finish temperature of the B2→R transition, B2→R→B19' - martensitic transformation, B19'→B2 - reverse martensitic transformation.

**TABELA 2. Temperatury przemian dla stopu NiTi.**  
**TABLE 2. Transformations temperatures of a NiTi alloy.**

A <sub>s</sub> [°C]	A <sub>f</sub> [°C]	M <sub>s</sub> [°C]	M <sub>f</sub> [°C]
-8.6	1.9	-22.3	-35.6

**TABELA 3. Temperatury przemian dla stopu NiTi z osadzoną warstwą ceramiki whitlockitowej po obróbce cieplnej w 1000°C przez 2 godziny.**  
**TABLE 3. Transformation temperatures of a NiTi alloy covered with whitlockite coating and heat-treated at 1000°C for 2 h.**

A <sub>s</sub> [°C]	A <sub>f</sub> [°C]	R <sub>s</sub> [°C]	R <sub>f</sub> [°C]	M <sub>s</sub> [°C]	M <sub>f</sub> [°C]
-2.1	7.0	4.2	-8.5	-37.6	-47.6

DSC results reveal reversible one-step and two-step martensitic transition with characteristic temperatures of the phase transformation below room temperature, respectively for initial NiTi sample (FIG. 4a, TABLE 2) and heat-treated at 1000°C per 2 h (FIG. 4b, TABLE 3). The starting NiTi alloy underwent a reversible martensitic transition with characteristic temperatures of martensitic transformation below room temperature. Both martensitic (B2→B19') and reverse martensitic transformation (B19'→B2) were one-step (FIG. 4a). DSC measurements performed for the sintered sample revealed that martensitic transformation occurred as a reversible one (FIG. 4b) what is a proof that the deposited coating do not block the transformation and the shape memory effect can be expected. Moreover, heat treatment changed the sequence of martensitic transformation from one- to two-step (FIG. 4). Transformation between the B2 parent phase and the monoclinic martensite B19' occurs thorough the R-phase during the cooling process.

## Conclusions

Application of deposition voltage of 20 V for 60 s resulted in homogenous covering of passivated NiTi substrate by whitlockite layer. As a result of heat-treatment (1000°C / 2 h in vacuum) crystallization of titanium oxides and partial decomposition of NiTi alloy were observed. However, the structure of CaP coating material remained unchanged.

Deposited CaPs agglomerates had thickness of about 5.6 μm. DSC measurements revealed lack of negative effect of the deposited whitlockite coating on the martensitic transformation in NiTi alloy, responsible for shape memory effect.

## Acknowledgements

*This work was supported by the Young Scientist Project (No. 1M-0817-001-1-10).*

## References

- [1] Morawiec H., Lekston Z.: *Implanty medyczne z pamięcią kształtu*. Wyd. Politechniki Śląskiej, Gliwice 2010.
- [2] Yoneyama T., Miyazaki S.: *Shape memory Alloys for biomedical applications*, Woodhead Publishing Limited, Cambridge 2009.
- [3] Es-Souni M., Es-Souni M., Fischer-Brandies H.: Assessing the biocompatibility of NiTi shape memory alloys used for medical applications. *Anal Bioanal Chem* 381 (2005) 557-567.
- [4] Shabalovskaya S. A., Anderegg J., Van Humbeeck J.: Critical overview of Nitinol surfaces and their modifications for medical applications. *Acta Biomater* 4 (2008) 447-467.
- [5] Sun F., Sask K., Brash J. L., Zhitomirsky I.: Surface modification of Nitinol for biomedical applications. *Colloid Surface B* 67 (2008) 132-139.
- [6] J. Lelątko, T. Goryczka: *Modyfikacja powierzchni stopów NiTi wykazujących pamięć kształtu*. Oficyna Wydawnicza WW, Katowice (2013).
- [7] D. Krause, B. Thomasa, Ch. Leinenbach, D. Eifler, E.J. Minay, A.R. Boccaccini: The electrophoretic deposition of Bioglass particles on stainless steel and Nitinol substrates. *Surface & Coatings Technology* 200 (2006) 4835-4845.
- [8] Dorozhkin S.V.: Calcium Orthophosphates in Nature. *Biology and Medicine, Materials* 2 (2009) 399-498.
- [9] Malysheva A.Yu., Beletskii B.I.: Biocompatibility of Apatite-Containing Implant Materials. *Inor Mater Vol.37 No.2* (2001) 180-183.
- [10] Horowitz R.A., Mazor Z., Foitzik Ch., Prasad H., Rohrer M., Palti A.: β-Tricalcium Phosphate as Bone Substitute Material: Properties and Clinical Applications. *Titanium* (2009) 2-11.
- [11] Dorozhkin S.V.: Calcium orthophosphate coatings, films and layers. *Progress in Biomaterials* (2012) 2-40.
- [12] Boccaccini R., Keim S., Ma R., Li Y., Zhitomirsky I.: Electrophoretic deposition of biomaterials, *J R Soc Interface* 7 (2010) S580-S613.
- [13] Zhitomirsky I.: Cathodic electrodeposition of ceramic and organoceramic materials. *Fundamental aspects, Adv Colloid Interfac* 97 (2002) 279-317
- [14] T. Goryczka, K. Dudek: Structure of multi-functional calcium phosphates/TiO<sub>2</sub> layers deposited on NiTi shape-memory alloy. *Powder Diffraction* (in press, DOI: 10.1017/S0885715617000239)
- [15] O. Albayrak, O. El-Atwani, S. Altintas: Hydroxyapatite coating on titanium substrate by electrophoretic deposition method: Effects of titanium dioxide inner layer on adhesion strength and hydroxyapatite decomposition. *Surface & Coatings Technology* 202 (2008) 2482-2487.
- [16] K. Dudek, M. Plawecki, M. Dulski, J. Kubacki: Multifunctional layers formation on the surface of NiTi SMA during β-tricalcium phosphate deposition. *Materials Letters* 157 (2015) 295-298.
- [17] K. Dudek, T. Goryczka: Electrophoretic deposition and characterization of thin hydroxyapatite coatings formed on the surface of NiTi shape memory alloy. *Ceramics International* 42 (2016) 19133-19141.
- [18] A. B. Jr. Novaes, S. L. de Souza, R. R. de Barros, K. K. Pereira, G. Iezzi, A. Piattelli: Influence of implant surfaces on osseointegration. *Brazilian Dental Journal* 21 (6) (2010) 471-481.

# MODIFICATION OF PLGA MICROSPHERES' MICROSTRUCTURE FOR APPLICATION AS CELL CARRIERS IN MODULAR TISSUE ENGINEERING

BARTOSZ MIELAN\*, MAŁGORZATA KROK-BORKOWICZ,  
KINGA PIELICHOWSKA, ELŻBIETA PAMUŁA

AGH UNIVERSITY OF SCIENCE AND TECHNOLOGY,  
FACULTY OF MATERIALS SCIENCE AND CERAMICS,  
DEPARTMENT OF BIOMATERIALS AND COMPOSITES,  
AL. MICKIEWICZA 30, 30-059 KRAKÓW, POLAND  
\*E-MAIL: BARMIE@AGH.EDU.PL

## Abstract

*Microspheres (MS) made of resorbable polymer have been proposed as a cell growth support. They may be assembled to form cell constructs or be suspended in hydrogels allowing injection into injury location. High relative surface area of MS provides more efficient cell culture environment than traditional culture on flat substrates (multiwell plates, Petri dishes). In addition, MS structure, topography and surface chemistry can be modified to promote cell adhesion and proliferation. The aim of this study was to obtain resorbable poly(L-lactide-co-glycolide) (PLGA) MS and to modify their properties by changing manufacturing conditions of the oil-in-water emulsification to better control structural and microstructural properties of MS and their biological performance. To this end, water phase was modified by addition of NaCl to change ionic strength, while oil phase by addition of polyethylene glycol (PEG). Microstructural and thermal properties were assessed. Cytocompatibility tests and cell cultures with MG-63 cells were conducted to verify potential relevance of MS as cell carriers. The results showed that it is possible to obtain cytocompatible MS by oil-in-water emulsification method and to control diameter, porosity and crystallinity of MS with the use of additives to oil and/or water phases without negative changes in MS cytocompatibility. The results prove that modification of both phases make it possible to produce MS with desired/controllable properties like surface topography, porosity and crystallinity.*

**Keywords:** regenerative medicine, cell cultures, bottom-up, PLGA, emulsification

[*Engineering of Biomaterials* 140 (2017) 7-11]

## Introduction

Due to high complexity of natural tissues and the need to treat tissue defects and diseases there is a growing interest in tissue engineering (TE) methods. Classical TE, called also top-down TE, uses cells, biologically active molecules and scaffolds to reconstruct tissues *in vitro* or *in vivo*. Conventional scaffolds are macroscopic devices made of different biomaterials which act as artificial extracellular matrices. Scaffolds seeded with cells have a limited ability to mimic natural tissues because they require proper open porosity to let regenerating tissue ingrowth, and cells need nutrients and exchange of many substances to promote angiogenesis, which is essential for wound healing [1].

Modular TE is a new approach called also bottom-up TE, that aims to resolve some problems of conventional top-down TE. Modular TE uses small units like e.g. microspheres, cell sheets, cell aggregates or cell laden modules to build bigger cell-tissue constructs on a way of self-assembly, aggregation or 3D printing [1,2]. This bottom-up TE approach allows to manipulate precisely with cells to combine small elements into more complex tissue systems [3,4].

MS used as cell microcarriers have the main advantage: cells can readily attach to their external surface and relatively high cell density can be achieved after cell culture [1]. Depending on application it is possible to obtain solid or porous MS [5]. Coupling proper porosity and high surface area with growth factors allows to obtain MS with appropriate properties for regenerating tissue [5]. Due to their spherical shape cells can grow in three dimensions [6]. Moreover MS can be suspended in hydrogels and injected into required place in the body [7]. The surface of MS may be modified by other substances like chitosan, fibronectin or collagen to improve cell adhesion and growth [6,8]. Additionally MS can be used to encapsulate drugs and growth factors [8] or be loaded with magnetic particles [9].

Diameter of MS may be controlled by factors like polymer type, properties as well as synthesis method and conditions. Majority of proposed in literature MS for cell growth have diameter between 100-250  $\mu\text{m}$  and are characterized by hydrophilic surface properties [10]. They are usually produced by oil-in-water emulsification. Microspheres size may be controlled by modification of aqueous phase with other substances (e.g. glucose) [9], concentration of polymer in oil phase or stirring speed of water phase [6]. Concentration of emulsion stabilizer, e.g. polyvinyl alcohol (PVA) in water phase also can influence diameter and shape of MS [11]. We hypothesize that modification of ionic strength of water phase by addition of non-toxic NaCl may result in MS with different structure and properties.

The aim of this study was to modify PLGA MS properties by changing manufacturing conditions and composition of oil-in-water emulsification phases to better control structural and microstructural properties of MS and their biological performance. To this end, water phase was modified by addition of NaCl to change ionic strength, while oil phase by addition of polyethylene glycol (PEG) intended to act as a pore former. PLGA being a matrix material was used due to its excellent biological properties and adaptable degradation time, which may be controlled by a ratio of lactide to glycolide and molecular mass.

## Materials and Methods

To obtain MS PLGA with molar ratio of L-lactide to glycolide of 85:15,  $M_n = 100$  kDa,  $M_w = 210$  kDa was dissolved in dichloromethane (DCM, Sigma-Aldrich) at a concentration of 20% wt/vol to create oil phase. Water phase was obtained by dissolving 1.5% poly(vinyl alcohol) (PVA) (Mowiol® 4-88,  $M_w = \sim 31,000$ , Sigma Aldrich) in ultra-high quality water (UHQ-water, produced by PureLab, Elga, UK). Three types of MS were obtained: MS1, MS2 and MS3. Reference MS1 were prepared by pouring 1 ml oil phase into 40 ml water phase under stirring on a magnetic stirrer (250 rpm). During injection of oil phase into water phase the tip of the pipette was 0.5 cm above the surface of the water phase. MS2 were produced in the same manner but water phase was supplemented with 0.5% NaCl. For MS3 manufacturing oil phase was modified by addition of 20% PEG ( $M_n = 400$  Da, Sigma-Aldrich). After 24 h the DCM was evaporated and MS were formed, vacuum filtered, rinsed with UHQ-water, dried at 37°C for 24 h, sieved and fraction  $>100$   $\mu\text{m}$  was collected. Manufacturing procedure is shown in FIG. 1.

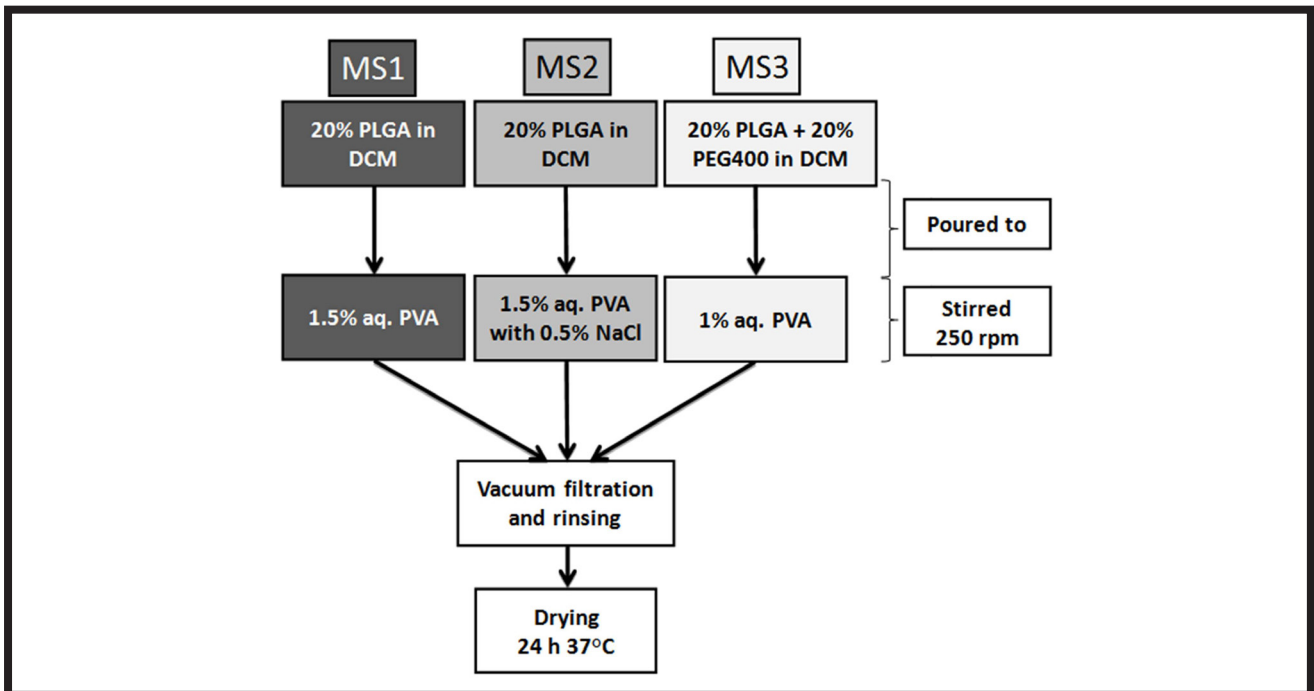


FIG. 1. Manufacturing conditions of PLGA microspheres: MS1, MS2, MS3 by oil-in-water emulsification.

TABLE 1. Microstructural properties of PLGA MS.

Sample	Diameter (mean $\pm$ S.D) $\mu\text{m}$	Diameter (median) $\mu\text{m}$	Shape factor
MS1	123.0 $\pm$ 22.0	120.2	1.04 $\pm$ 0.06
MS2	134.2 $\pm$ 22.5	132.6	1.03 $\pm$ 0.06
MS3	127.5 $\pm$ 21.8	124.8	1.04 $\pm$ 0.08

MS were analysed with optical microscopes (Axiovert 40, Zeiss and VHX-900F, Keyence), scanning electron microscope (Nano Nova SEM 200) and differential scanning calorimetry (DSC, DSC1 from Mettler Toledo). DSC measurements were performed in the temperature range of  $-90$ – $200^\circ\text{C}$  at heating rate of  $10^\circ\text{C}/\text{min}$  in nitrogen atmosphere; sample mass was ca. 6 mg. To measure glass transition temperature ( $T_g$ ) TOPEM DSC was used with reversing heat flow. To assess size, size distribution and shape factor 300 individual MS were measured from each group with the use of AxioVision software provided with the optical microscope (Axiovert 40, Zeiss).

Before cell culture tests the MS samples were sterilized in ethanol in 48-well plates (Nunclon; 8 mg MS dispersed in 200  $\mu\text{l}$  70% ethanol was poured into each well). After ethanol evaporation (24 h under laminar hood) MG-63 osteoblast-like cells suspension ( $5 \times 10^3$  cells/well) in 500  $\mu\text{l}$  MEM supplemented with 10% fetal bovine serum, 1% penicillin/streptomycin, 2 mM L-glutamine (PAA, Austria) was added to each well and cells were cultured at  $37^\circ\text{C}$  and 5%  $\text{CO}_2$ . Empty cell culture wells (tissue culture polystyrene, TCPS) acted as control. After 1 and 3 days Alamar Blue assay (Sigma Aldrich) was performed. After 1, 3 and 7 days the cells were stained for live/dead (calcein AM/propidium iodide, Sigma Aldrich) and observed under fluorescence microscope (Axiovert, Zeiss).

## Results and Discussion

The aim of this work was to obtain PLGA MS with diameter above 100  $\mu\text{m}$  and with size distribution as narrow as possible and regular spherical shape. Independently from manufacturing parameters average diameter of all microspheres was similar (FIG. 2 A, B, C). MS1 had diameter of  $123.0 \pm 22.0 \mu\text{m}$ , median 120.2  $\mu\text{m}$ , MS2 had diameter of  $134.2 \pm 22.5 \mu\text{m}$ , median 132.6, while the diameter of MS3 was  $127.5 \pm 21.8 \mu\text{m}$ , median 124.8  $\mu\text{m}$ ; no significant differences were found according to ANOVA. Also shape factor of all the samples was similar and relatively low (TABLE 1). Distribution of diameters was similar for all the samples (FIG. 2 A, B, C).

Optical microscopy observations (FIG. 2 D, E, F) revealed significant differences between microspheres: MS2 were the most transparent of all examined samples, while MS3 were the most opaque. SEM pictures (FIG. 2 G) showed that MS1 had small pores (few micrometers in diameter) on the surface and were the most rough, while MS2 and MS3 were smooth on the surface (FIG. 2 H, I, respectively).

FIG. 3 shows DSC curves, while TABLE 2 thermal properties of PLGA MS. It is apparent that all MS had similar melting temperature,  $T_m$ , ca.  $134^\circ\text{C}$  but different melting enthalpy ( $\Delta H_m$ ): MS2 had the lowest  $\Delta H_m$ , while MS3, the highest. Also glass transition temperature,  $T_g$ , of MS2 was the lowest, while for MS3 the highest. The degree of crystallinity,  $X$ , was calculated from the measured heat of melting, using the value of heat of melting of the crystalline regions of poly-L-lactide,  $\Delta H_m = 93.1 \text{ J/g}$  [12], taking into account that in PLGA content of L-lactide was 85%. The results show that the degree of crystallinity of 1.25% was found for MS2, while 6.1% for MS3.

*In vitro* tests showed that the cells adhered and grew on MS. Observations under fluorescence microscope showed that the cells grew both on TCPS wells and on MS irrespectively of the type of MS (FIG. 2 J, K, L). Majority of the cells were alive (stained green) and only less than 5% cells were dead (stained red). Cell viability after day 1 was significantly different between MS1 and MS2 as well as MS2 and MS3 as shown by Alamar Blue test (FIG. 4).

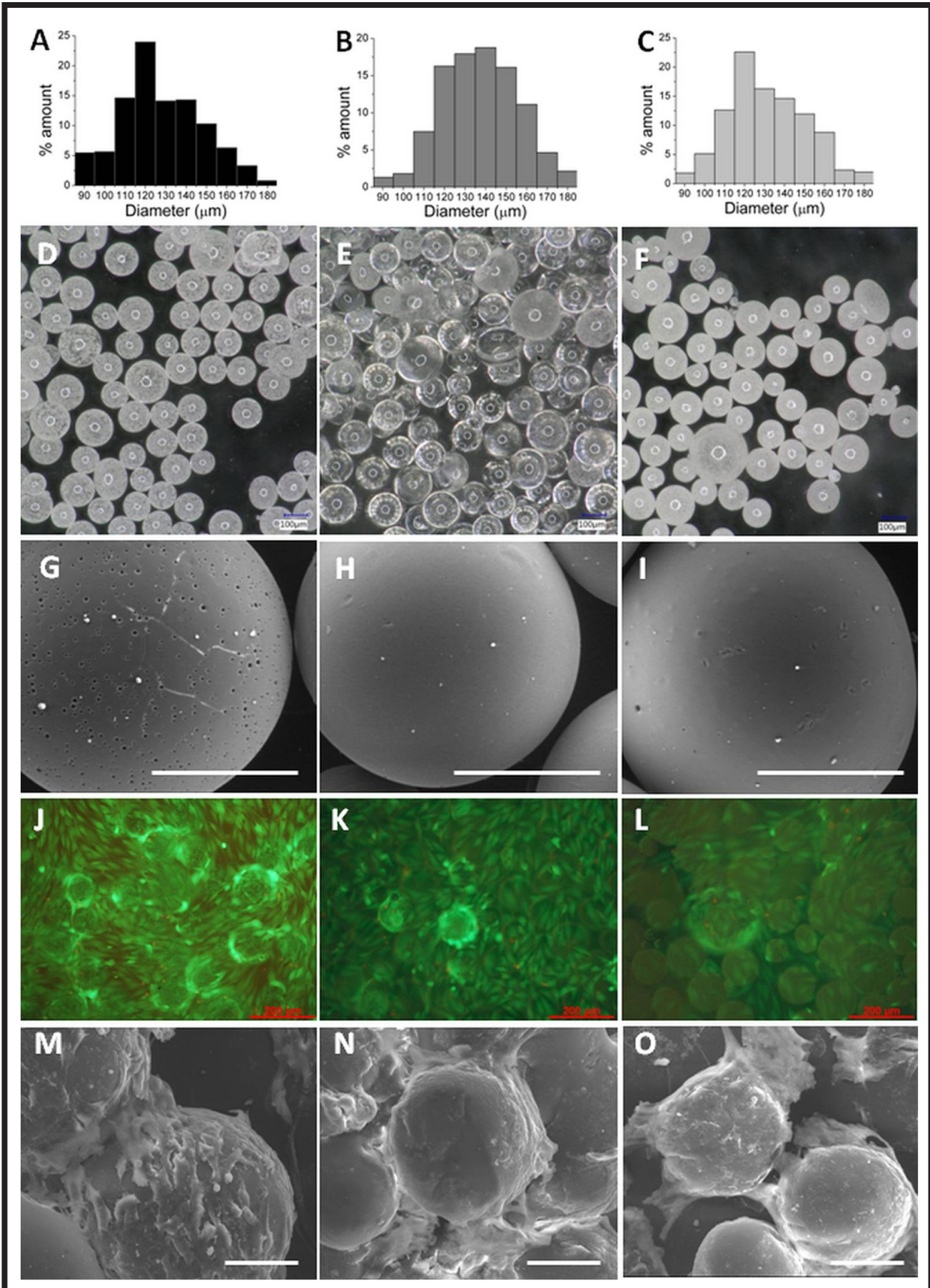


**FIG. 2.** Histograms of size distribution of MS1 (A), MS2 (B), MS3 (C); optical microscopy images of MS1 (D), MS2 (E), MS3 (F); SEM microphotographs of MS1 (G), MS2 (H), MS3 (I) (scale bar 50  $\mu\text{m}$ ); live/dead staining images after 7-day cell culture on MS1 (J), MS2 (K), MS3 (L) and SEM microphotographs of cells after 7-day cell culture on MS1 (M), MS2 (N), MS3 (O) (scale bar 50  $\mu\text{m}$ ).

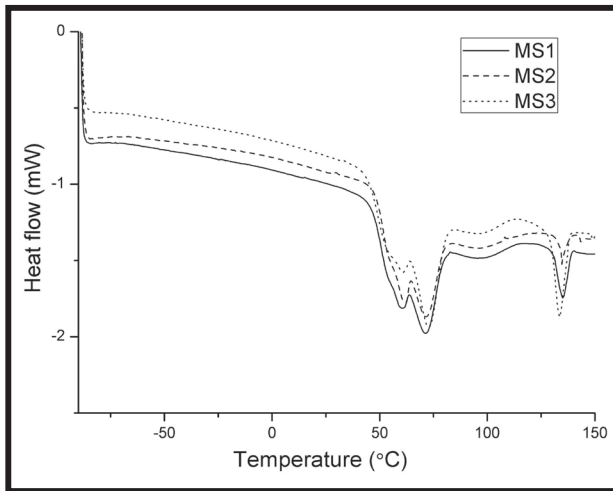


FIG. 3. DSC curves of MS1, MS2 and MS3.

TABLE 2. Thermal properties of MS.

Sample	$T_g$ °C	$T_m$ °C	Melting enthalpy $\Delta H_m$ J/g	Crystallinity X %
MS1	54.8	135.09	- 2.47	3.1
MS2	49.0	134.60	- 0.92	1.2
MS3	55.8	133.41	- 4.82	6.1

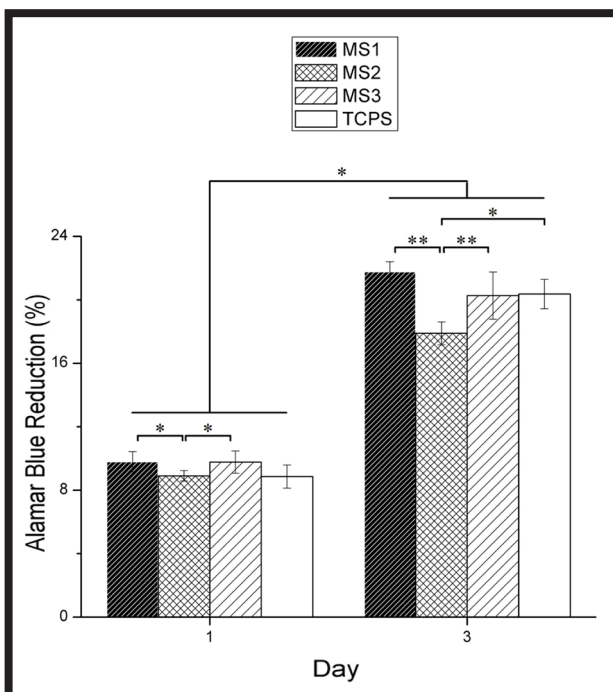


FIG. 4. MG-63 cell viability studied by Alamar Blue reduction on day 1 and 3, no significant differences was found between the samples on the same day, significant difference \* $p < 0.01$ , \*\* $p < 0.05$  according to ANOVA.

On day 3 the viability of cells increased but the lowest viability of cells was on MS2. SEM observations show morphology of the cells cultured on the scaffolds (FIG. 1 M, N, O). It is apparent that the cells adhered well on MPS and in some cases formed monolayers. Some of the cells adhered to two or three MS, as a result the agglomerates were formed.

In this study the aim was to produce PLGA MS by oil-in-water emulsification and to verify if compositions of water and oil phases influence microstructure, thermal and biological properties of resulting MS.

It was found that all MS had the same diameter of 120-130  $\mu\text{m}$  and were of regular shape; shape factor equal to 1.03 – 1.04 was similar to all microspheres. Interestingly, modification of water phase (MS2) and oil phase (MS3) resulted in differences in appearance, transparency, microstructure and thermal properties of the MS. Addition of NaCl to water phase caused high transparency and low porosity of MS2. When oil phase was modified with PEG400 opposite effect was observed: MS3 were opaque. Opacity of MS3 results from higher crystallinity of PLGA as shown by DSC studies – polymer crystallites cause light scattering. Microstructure of MS differed between samples and depended on the used modification approaches but in general the surface of MS was smooth and small pores (few  $\mu\text{m}$  in diameter) were found on non-modified MS1.

It was found that modification of water phase with NaCl, which increased its ionic strength, resulted in more amorphous PLGA forming MS. Presence of NaCl, which can be occluded between macrochains of PLGA, had an impact on  $T_g$  and crystallinity, what suggests that sodium and chloride ions acted as plasticizer for PLGA, by increasing the distance between polymer microchains. Addition of PEG to PLGA solution in DCM (modification of oil phase) resulted in increase in crystallinity of MS, probably due to the fact that PLGA and PEG did not form a physical mixture but undergo phase separation as shown in our previous study [13]. The second reason might be that PEG chains can interact with PLGA macrochains with hydrogen bonds, which increase  $T_g$ ,  $T_m$  and enhance formation of more organized, crystalline phases. The findings regarding crystallinity are important from the point of view of using MS in cell culture, because it is known that crystallinity influences degradation kinetics of PLGA.

Irrespectively of differences in crystallinity *in vitro* tests proved good cytocompatibility of all investigated MS. Alamar Blue assay showed that the best cell supporting properties were found for MS1 and MS3. Live/dead staining showed that adhesion of cells on MS surface after 7 days was high and a vast majority of the cells were alive (>95%). Additionally SEM microphotographs showed that microspheres with cells tended to form agglomerates what additionally proved high cell compatibility of tested MS.

## Conclusions

Obtained results demonstrate that it is possible to obtain microspheres with defined properties like porosity, size and crystallinity by controlling emulsification process parameters with additions of chemicals to oil or water phases. All MS were cytocompatible what allows to consider them as cell carriers in modular tissue engineering.

## Acknowledgements

This study was financed from National Science Center, Poland (UMO-2016/21/D/ST8/0185).

## References

- [1] Ciucurel E.C., Chamberlain M.D., Sefton M.V.: Chapter 7: The Modular Approach. In: Biofabrication (2013) 119-148.
- [2] Nichol J.W., Khademhosseini A.: Modular tissue engineering : engineering biological tissues from the bottom up. *Soft Matter*: 5 (2007) 1312-1319.
- [3] Yang W., Yu H., Li G., Wang Y., Liu L.: High-Throughput Fabrication and Modular Assembly of 3D Heterogeneous Microscale Tissues. *Small* 13 (2017) 1-11.
- [4] Cvetkovic C., Rich M.H., Raman R, Kong H., Bashir R.: A 3D-printed platform for modular neuromuscular motor units. *Microsystems & Nanoengineering*: 3 (2017) 1-9.
- [5] Hossain K.M.Z., Patel U., Ahmed I.: Development of microspheres for biomedical applications : a review. *Prog Biomater*: 4 (2015) 1-19.
- [6] Gabler F., Frauenschuh S., Ringe J., Brochhausen C., Götz P., Kirkpatrick C.J., Sittinger M., Schubert H., Zehbe R.: Emulsion-based synthesis of PLGA-microspheres for the *in vitro* expansion of porcine chondrocytes. *Biomolecular Engineering*: 24 (2007) 515-520.
- [7] Schon B.S., Hooper G.J., Woodfield T.B.F.: Modular Tissue Assembly Strategies for Biofabrication of Engineered Cartilage 45 (2017) 100-114.
- [8] Lao L., Tan H., Wang Y., Gao C.: Chitosan modified poly (L-lactide) microspheres as cell microcarriers for cartilage tissue engineering. *Colloids and Surfaces B: Biointerfaces* 66 (2008) 218-225.
- [9] Hu L., Huang M, Wang J., Zhong Y., Luo Y.: Preparation of magnetic poly(lactic-co-glycolic acid) microspheres with a controllable particle size based on a composite emulsion and their release properties for curcumin loading. *Journal of Applied Polymer Science* 133 (2016) 1-8.
- [10] Bardouille C., Lehmann J., Heimann P., Jockusch H.: Growth and differentiation of permanent and secondary mouse myogenic cell lines on microcarriers. *Appl Microbiol Biotechnol* 55 (2001) 556-562.
- [11] Jeong Y.I., Song J.G., Kang S.S., Ryu H.H., Lee Y.H., Choi C., Shin B.A., Kim K.K., Ahn K.Y., Jung S.: Preparation of poly(DL-lactide-co-glycolide) microspheres encapsulating all-trans retinoic acid. *International Journal of Pharmaceutics* 259 (2003) 79-91.
- [12] Liu X., Wang T., Chow L.C., Yang M., Mitchell J.W.: Effects of Inorganic Fillers on the Thermal and Mechanical Properties of Poly(lactic acid). *International Journal of Polymer Science* (2014) 1-8.
- [13] Krok M., Pamuła E.: Poly(L-lactide-co-glycolide) microporous membranes for medical applications produced with the use of polyethylene glycol as a pore former. *J Appl Polym Sci* 125 (2012) 187-199.

# DETONATION NANODIAMOND PARTICLES MODIFIED BY NON-STEROIDAL ANTI-INFLAMMATORY DRUGS *IN VITRO* EXAMINATION

KATARZYNA MITURA<sup>1\*</sup>, PIOTR WILCZEK<sup>2</sup>,  
ALEKSANDRA NIEMIEC-CYGANEK<sup>2</sup>, MAŁGORZATA MORENC<sup>2</sup>,  
MARIUSZ DUDEK<sup>3</sup>, ANNA SOBCZYK-GUZENDA<sup>3</sup>,  
JUSTYNA FRACZYK<sup>4</sup>, BEATA KOLESIŃSKA<sup>4</sup>

<sup>1</sup> KOSZALIN UNIVERSITY OF TECHNOLOGY,  
DEPARTMENT OF BIOMEDICAL ENGINEERING,  
ŚNIADECKICH 2,75-453 KOSZALIN, POLAND

<sup>2</sup> FOUNDATION OF CARDIAC SURGERY DEVELOPMENT,  
WOLNOŚCI 345A, 41-800 ZABRZE, POLAND

<sup>3</sup> LODZ UNIVERSITY OF TECHNOLOGY,  
INSTITUTE OF MATERIALS SCIENCE AND ENGINEERING,  
STEFANOWSKIEGO 1/15, 90-924 LODZ, POLAND

<sup>4</sup> LODZ UNIVERSITY OF TECHNOLOGY, FACULTY OF CHEMISTRY,  
INSTITUTE OF ORGANIC CHEMISTRY,  
ŻEROMSKIEGO 116, 90-924 LODZ, POLAND

\* E-MAIL: MITURA.KATARZYNA@GMAIL.COM

## Abstract

*Most recently it has been found that nanodiamond particles have very interesting properties. There are number of research communications that detonation nanodiamond particles (NDPs) are fairly reactive and their surface can be effectively modified by chemical methods. The hydroxyl-modified NDPs were obtained by Fenton reaction, amine-functionalized NDPs were obtained by chemical reduction of the nitro-functionalized surface and carboxyl-modified NDPs by oxidation by using H<sub>2</sub>O<sub>2</sub> under acidic conditions. NDPs functionalized by hydroxyl- and amine- groups and amino groups were used for covalent binding of non-steroidal anti-inflammatory pharmaceuticals (aspirin, ketoprofen, ibuprofen, naproxen) via ester or amide bonds. These results of the studies proved the activity of the conjugates of active substance-NDP and study the rate of release of active substance from the NDPs surface by *in vitro* examinations with mouse fibroblasts.*

*The progress of the reaction and the characteristics of the products were determined by using FT-IR. Chemical and physical structures of materials were also investigated by Diffuse Reflectance Infrared Fourier Transform Spectroscopy (DRIFTS). DRIFT spectra show the modification of nanodiamond by ketoprofen, naproxen, ibuprofen and aspirin.*

**Keywords:** detonation nanodiamond particles, chemical modification, anti-inflammatory drugs, FT-IR spectroscopy, mouse fibroblasts

[*Engineering of Biomaterials 140 (2017) 12-20*]

This article was presented at 10<sup>th</sup> International Forum on Innovative Technologies for Medicine – ITMED, 7-9 November 2016, Warsaw, Poland.

## Introduction

Recent studies on application of carbon nanomaterials for biological purposes revealed that nanodiamonds are much more biocompatible than other carbon nanomaterials. The non-cytotoxic properties of nanodiamond particles together with other properties make them attractive for various biomedical applications both *in vitro* and *in vivo* [1]. Nanodiamond particles possess a unique set of properties attractive for drug delivery applications, including exceptional biocompatibility, large carrier capacity and versatile surface chemistry properties, which enhance drug binding and provide sustainable drug release.

Nanodiamond particles were obtained using Danilenko detonation method (discovered in 1963 in Soviet Union [2]) from graphite in presence oxygen-deficient TNT (2-methyl-1,3,5-trinitrobenzene)/hexogen composition in inert media. Detonation nanodiamond consists of nanodiamond particles (grain size from 2 to 10 nm), but the particles tend to aggregate [2-4]. Detonation nanodiamond particles are hydrophilic and nanodiamond surface has the many dangling bonds, which are chemically reactive and ready for chemical functionalization [5-9].

Detonation nanodiamond particles obtained by detonation method are described in the literature as the so-called "onion-like carbon" (OLC) [10-12]. Due to the nanoscale size of e.g. detonation nanodiamond particles, such material can be used for biological studies [13,14]. The series of research began by checking the biological properties of nanodiamond particles, which differ in content of a diamond phase and a grain size [15].

Nanodiamond particles modified by Fenton reaction exhibit the phenomenon of fluorescence in the presence of a strain of *Pseudomonas aeruginosa* ATCC 9027 that can be used in microbiological diagnostics packages containing diamond nanoparticles [6].

Detonation nanodiamond particles functionalized with hydroxyl groups were verified in studies evaluating their antioxidant potential. Detonation nanodiamond particles delayed soybean oil from going rancid, which is important in the potential for using them in bioactive packaging extending the period of food consumption [7].

Functionalization of pristine nanodiamond (ND) has influenced on fragmentation of nanoparticles, wettability and intensify of catalytic properties. Oxidation of the particle surface results in the possibility of selective attachment of functional groups and molecules. The internal carboxylic groups were observed on the nanodiamond surface. Thanks to their presence, further modifications can be made through the amide linkage. In this way the surface is modified with attached amines. Chemical modification of nanodiamond by amide functionalization increased hydrophilicity of the surface. Hydrophilicity (measured by dispersibility test in water and alcohol) makes nanodiamond surface susceptible to chemical modifications which can be controlled and selected for their medical applications [16].

Modern methods of tissue engineering utilize the acellular scaffolds *ex vivo* or *in vivo* seeded with the cells. Such scaffolds must be biocompatible, athrombogenic and mechanically stable. Often the factors used for the scaffold decellularization may affect the properties of the scaffolds cause the morphological and biomechanical changes within the extracellular matrix [17-19]. Therefore, the methods which improve the biocompatibility and mechanical properties of the materials used for bioprosthesis preparation are sought. For this purpose, nanodiamonds that show promising biological properties may be used [20-24]. The aim of the study was to assess the cytotoxicity of the nanodiamonds conjugated with the anti-inflammatory factors.

## Materials and Methods

### Methodology of chemical modification of detonation nanodiamond particles

#### Synthesis of nitro-modified NDP 2

Purified in ethanol nanodiamond powder (1.1 g) was placed into round bottom flask and 22 ml of 90% HNO<sub>3</sub> was added. The suspension was sonicated in a series of 20 x 5 min and intensively mixed on a magnetic stirrer for 72 h at room temperature. The precipitate was filtered off and washed with water until neutral pH. Modified NO<sub>2</sub>-NDP was dried in a vacuum desiccator to constant weight and finally 1.07 g modified NO<sub>2</sub>-NDPs **2** was obtained.

#### Synthesis of amino-modified NDP 3

Nitro-modified NDP (NO<sub>2</sub>-NDP, 1 g) was thoroughly triturated in a mortar with FeSO<sub>4</sub> (2.4 g). The powder was placed into round bottom flask and 100 ml of a mixture of ethane-water (1:1) was added. Vigorously stirred suspension was refluxed for 30 min. After cooling to room temperature, a further portion of FeSO<sub>4</sub> (5 g) and ethanol (10 ml) was added to suspension. Vigorously stirred suspension was refluxed for 1 h. After cooling to room temperature, solution of ammonia (80 ml) was added to suspension. Vigorously stirred suspension was refluxed for 5 h. In the next step FeSO<sub>4</sub> (5 g) was added to the suspension and it was refluxed for 1 h. After this time, solution of ammonia (80 ml) was added once again to the suspension and vigorously stirred; suspension was refluxed for 3 h. The suspension was diluted with water (100 ml) and the precipitate was filtered under reduced pressure. The precipitate was washed with water (25 ml), 5% H<sub>2</sub>SO<sub>4</sub> (25 ml), water (50 ml) and 10% NaOH (25 ml). The final product was dried in a vacuum desiccator to a constant weight.

#### Synthesis of triazine esters of carboxylic acids 6a-d.

##### General procedure

Carboxylic acid (1 mmol) and DIPEA (88  $\mu$ L, 0.5 mmol) were added at 0°C to a vigorously stirred solution of DMT/NMM/TosO<sup>-</sup> **5** (0.413 g, 1 mmol) in CH<sub>2</sub>Cl<sub>2</sub> (5 mL). Stirring was continued until the disappearance of condensing reagent **5** (TLC analysis, staining with 0.5% solution of NBP), after the time the mixture was diluted with DMF (5 mL) and used without any isolation and purification in next steps of H<sub>2</sub>N-NDP **3** functionalizations.

#### Synthesis of triazine active ester 6a derived from Aspirin 4a

Synthesis was carried out according to the general procedure. Starting materials: Aspirin **4a** (0.180 g, 1 mmol), DMT/NMM/TosO<sup>-</sup> **5** (0.413 g, 1 mmol), DIPEA (88  $\mu$ L, 0.5 mmol), CH<sub>2</sub>Cl<sub>2</sub> (5 mL) and DMF (5 mL).

#### Synthesis of triazine active ester 6b derived from Ketoprofen 4b

Synthesis was carried out according to the general procedure. Starting materials: Ketoprofen **4b** (0.254 g, 1 mmol), DMT/NMM/TosO<sup>-</sup> **5** (0.413 g, 1 mmol), DIPEA (88  $\mu$ L, 0.5 mmol), CH<sub>2</sub>Cl<sub>2</sub> (5 mL) and DMF (5 mL).

#### Synthesis of triazine active ester 6c derived from Ibuprofen 4c

Synthesis was carried out according to the general procedure. Starting materials: Ibuprofen **4c** (0.206 g, 1 mmol), DMT/NMM/TosO<sup>-</sup> **5** (0.413 g, 1 mmol), DIPEA (88  $\mu$ L, 0.5 mmol), CH<sub>2</sub>Cl<sub>2</sub> (5 mL) and DMF (5 mL).

#### Synthesis of triazine active ester 6d derived from Naproxen 4d

Synthesis was carried out according to the general procedure. Starting materials: Naproxen **4d** (0.206 g, 1 mmol), DMT/NMM/TosO<sup>-</sup> **5** (0.413 g, 1 mmol), DIPEA (88  $\mu$ L, 0.5 mmol), CH<sub>2</sub>Cl<sub>2</sub> (5 mL) and DMF (5 mL).

#### Synthesis of NDPs 7a-d modified with carboxylic acid derivatives. General procedure

To a vigorously stirred and cooled in ice-water bath (0°C) suspension of H<sub>2</sub>N-NDP **3** (100 mg) in CH<sub>2</sub>Cl<sub>2</sub> (2 mL) was added a solution of the triazine ester **6** (1 mmol) and NMM (110  $\mu$ L, 1 mmol). Stirring was continued for 12 h at room temperature. The precipitate was filtered off under reduced pressure and thoroughly washed with DMF (10 mL), CH<sub>2</sub>Cl<sub>2</sub> (10 mL), water (10 mL), DMF (10 mL) and CH<sub>2</sub>Cl<sub>2</sub> (10 mL). The residue was dried to constant weight in a vacuum desiccator.

#### Synthesis of NDP 8 modified with $\beta$ -alanine residue.

##### General procedure

To a vigorously stirred and cooled in ice-water bath (0°C) suspension of H<sub>2</sub>N-NDP **3** (500 mg) in CH<sub>2</sub>Cl<sub>2</sub> (10 mL) was added a solution of DMT/NMM/TosO<sup>-</sup> **5** (2.65 g, 5 mmol), Fmoc- $\beta$ -Ala-OH (1.557 g, 5 mmol) and NMM (660  $\mu$ L, 6 mmol) in mixture of DMF and CH<sub>2</sub>Cl<sub>2</sub> (1:1) (15 mL). The experiment was continued for 12 h at room temperature. The precipitate was filtered off under reduced pressure and thoroughly washed with DMF (20 mL), CH<sub>2</sub>Cl<sub>2</sub> (20 mL), water (20 mL), DMF (10 mL) and CH<sub>2</sub>Cl<sub>2</sub> (20 mL). The residue was dried to a constant weight in a vacuum desiccator. The suspension of Fmoc- $\beta$ -Ala-NDP in DMF (5 ml) was added 25% solution of piperidine in DMF. The suspension was sonicated for 5 min and then vigorously stirred for 15 min on a magnetic stirrer. The suspension was centrifuged (15 min, 4000 rpm), the supernatant was decanted. To the precipitate 25% solution of piperidine in DMF was added again and all procedure was repeated three times. The precipitate was filtered off under reduced pressure and thoroughly washed with DMF (20 mL), CH<sub>2</sub>Cl<sub>2</sub> (20 mL), water (20 mL), DMF (10 mL) and CH<sub>2</sub>Cl<sub>2</sub> (20 mL). The residue was dried to constant weight in a vacuum desiccator.

#### Synthesis of NDPs 9a-d modified with carboxylic acid derivatives. General procedure

To a vigorously stirred and cooled in ice-water bath (0°C) suspension of H<sub>2</sub>N- $\beta$ -Ala-NDP **8** (100 mg) in CH<sub>2</sub>Cl<sub>2</sub> (2 mL) a solution of the triazine ester **6** (1 mmol) and NMM (110  $\mu$ L, 1 mmol) was added. Stirring was continued for 12 h at room temperature. The precipitate was filtered off under reduced pressure and thoroughly washed with DMF (10 mL), CH<sub>2</sub>Cl<sub>2</sub> (10 mL), water (10 mL), DMF (10 mL) and CH<sub>2</sub>Cl<sub>2</sub> (10 mL). The residue was dried to constant weight in a vacuum desiccator.

### FT-IR spectroscopy examination

The progress of the reaction and the characteristics of the products were determined by using FT-IR. All measurements were carried out at room temperature and in air atmosphere. Chemical and physical structures of materials were also investigated by Diffuse Reflectance Infrared Fourier Transform Spectroscopy (DRIFTS) using the Thermo Scientific Nicolet iS50 FT-IR spectroscope. DRIFT spectra were collected in the range of 400-4000 cm<sup>-1</sup>.

### Methodology of *in vitro* examination

To prevent cell culture contamination the diamond powders particles were exposed to solution containing antibiotics (100 U/ml Penicilin/Streptomycin, 5 mg/ml Ciprofloxacin and 2 mg/ml Fluconazolom) at 4°C for 24 h. Mouse fibroblasts L929 (ATCC CCL-1) were used for Cytotoxicity test. Cell cultivation was performed in medium 199 with 10% fetal bovine serum, 100 U/ml Penicilin/Streptomycin, 5 mg/ml Ciprofloxacin and 2 mg/ml Fluconazolom. The cells were growing at 37°C and 5% CO<sub>2</sub>. When fibroblasts reached 80% confluency they were treated with the diamond powder suspensions (50 µg/ml). Cell viability was assessed after 24 h using fluorescent microscope (Zeiss AxioObserver.Z1 fluorescence microscope, 10x). For that purpose fluorescent staining were used: fluorescein diacetate (FDA, 1 mg/ml) which penetrates through living cells membrane gives green fluorescence and propidium iodide which gives bright red light on apoptotic and necrotic cells. TABLE 1 showed methodological assumptions for the *in vitro* experiment.

## Results and Discussion

One of the most popular methods of functionalization of nanodiamond particles is the incorporation of hydroxyl groups on the surface of the nanoparticles under the Fenton reaction conditions [25]. The presence of hydroxyl groups on the surface of the NDPs enables their widespread adaptation in subsequent functionalization steps by using variety of molecules. The hydroxyl-modified nanodiamond particles were obtained by Fenton reaction, amine-functionalized NDPs by chemical reduction of the nitro-functionalized surface, carboxyl-modified NDPs by oxidation with the use of H<sub>2</sub>O<sub>2</sub> under acidic conditions [26].

However, direct transformation of hydroxyl groups with a carboxylic acid derivatives leads to the formation of the corresponding esters which under physiological conditions have a moderate stability. In order to eliminate the inconvenience of inadequate stability of NDPs modified with biologically active carboxylic acids (nonsteroidal anti-inflammatory drugs, NSAIDs), it has been assumed that the more stable are the corresponding amide derivatives.

Functionalization of NDPs surface by amino groups has been achieved in a two-steps reaction. The first reaction step involved the nitration of the NDPs surface under standard nitration conditions. In the second step the nitro groups were reduced to the corresponding amines [27] (FIG. 1).

The next step functionalization H<sub>2</sub>N-NDPS (**3**) consisted of the acylation of the amino functions on the surface of NDPs by super-active triazine esters **6** of NSAIDs (aspirin **4a**, ketoprofen **4b**, ibuprofen **4c** and naproxen **4d**) with 4-(4,6-dimethoxy-1,3,5-triazin-2-yl)-4-methylmorpholinium toluene-4-sulfonate (DMT/MMM/TosO<sup>-</sup> **5**) [27] (FIG. 2).

TABLE 1. The qualitative and morphological classification of cellular cytotoxicity.

Cytotoxicity	Reactivity	Cell condition
0	lack	Discrete intra-plasmatic granules, no lysis, no reduction of cell growth
1	slight	Not more than 20% of round cells, loosely adherent without intra-plasmatic granules, showing morphological changes, slight cell lysis, a slight inhibition of cell growth
2	mild	Not more than 50% of round cells, without intra-plasmatic granules, strong cell lysis, not more than 50% inhibition of cell growth
3	moderate	Not more than 70% a surface comprising a round and lysed cell, not completely damaged, cell growth inhibition more than 50%
4	strong	Almost total and complete destruction of cells

The choice of a triazine coupling reagents to modify the surface of NDPs was dictated by the fact that the acylation of nucleophiles with superactive triazine esters is very effective and application of them ensuring the removal of side-products (elimination of deposits on the surface of a solid matrix). 2-Hydroxy-4,4-dimethoxy-1,3,5-triazine, the side product of acylation with triazine based coupling reagents is removed by extraction with polar organic solvents or by washing with water.

In order to improve the exposition of NSAIDs on the surface of the nanoparticles modified NDPs containing the rest of β-alanine as a linker between the nanoparticles and attached NSAIDs were obtained (FIG. 3).

For the acylation of amino groups of NDPs **3** DMT/MMM/TosO<sup>-</sup> **5** as a coupling reagent was used. The coupling and subsequent removal of the Fmoc group has been done by using standard synthetic protocols for solid phase peptide synthesis [28]. The stage of incorporation of acid derivatives (NSAIDs) was implemented by using appropriate triazine esters **6a-d** derived from aspirin **4a**, ketoprofen **4b**, ibuprofen **4c** and naproxen **4d**.

FIGs 4-6 show the results of FT-IR spectroscopy of nanodiamond particles without chemical modification (FIG. 4) and the attached anti-inflammatory drugs (FIGs 5 and 6). The results of FT-IR confirm the presence of amide bonds (FIG. 5) and amide bonds by a β-alanine connector.

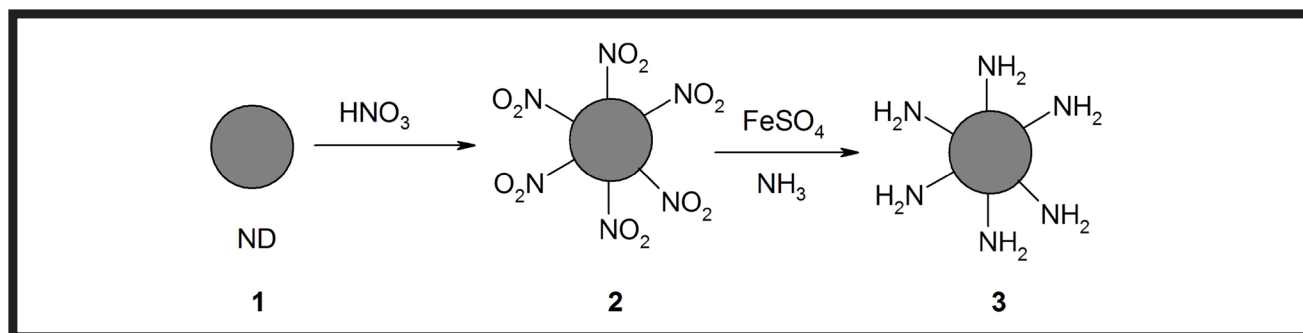


FIG. 1. Synthesis of amino-functionalized NDPs.

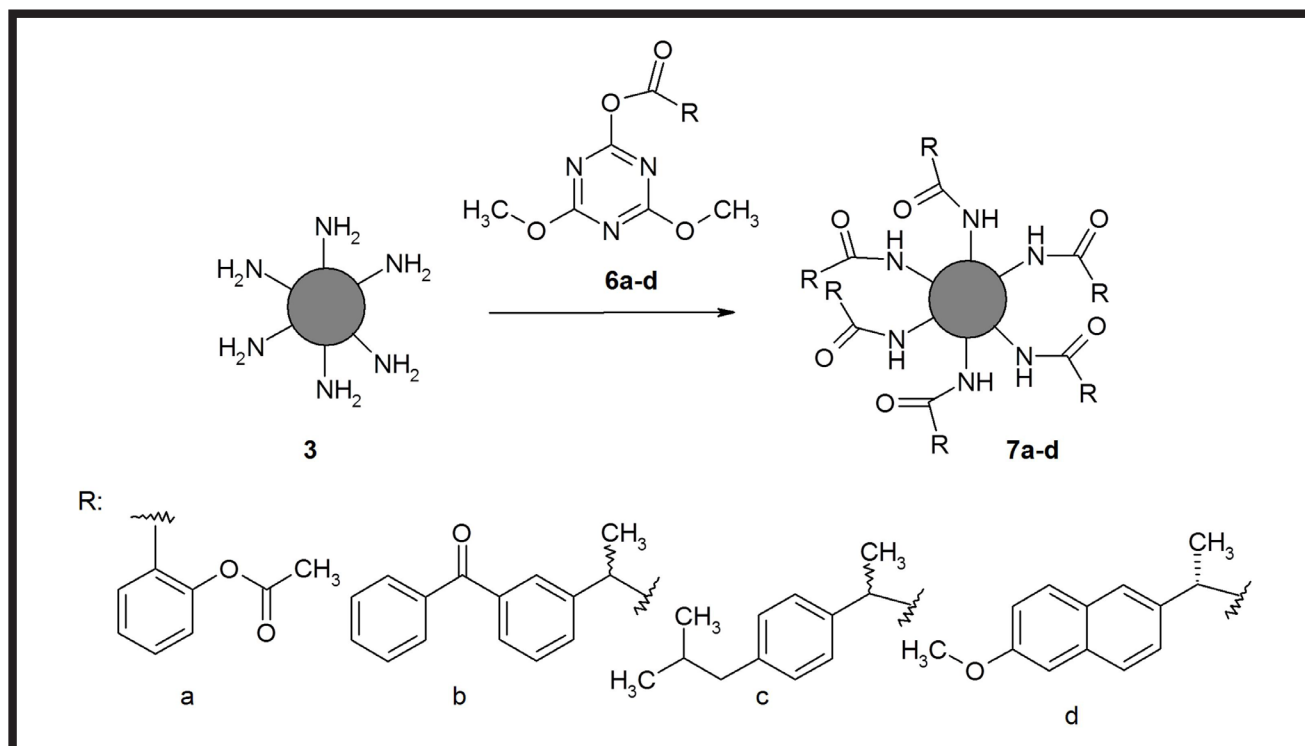


FIG. 2. Synthesis of NDPs 7a-d modified with nonsteroidal anti-inflammatory drugs.

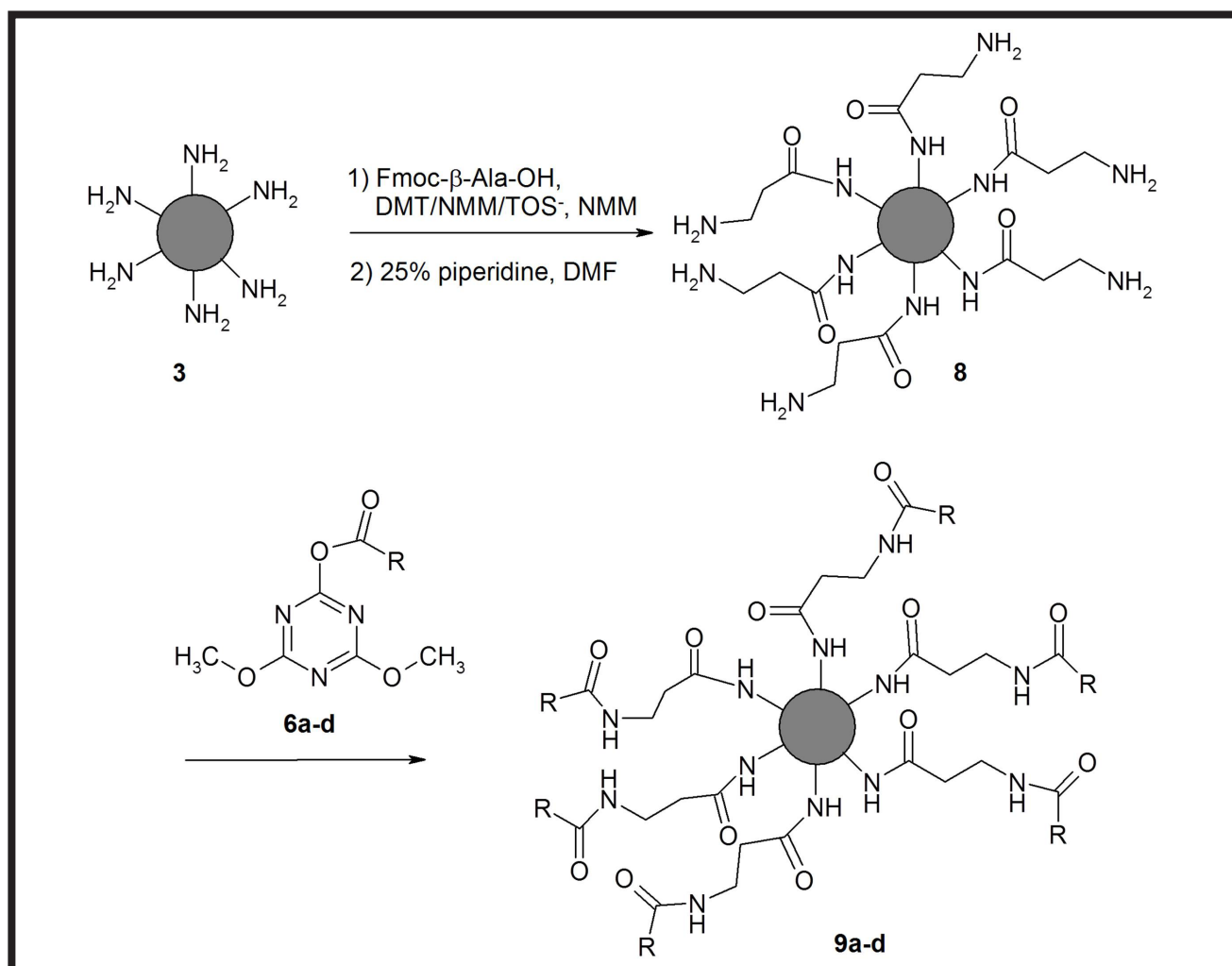


FIG. 3. Synthesis of NDPs 9a-d modified with nonsteroidal anti-inflammatory drugs separated from surface of nanoparticle by  $\beta$ -alanine residue.

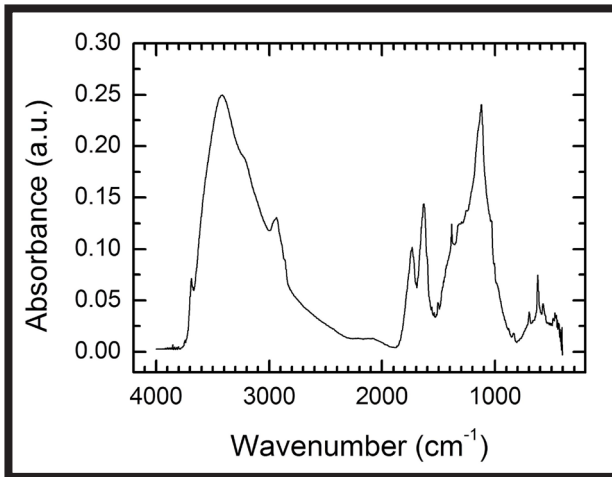


FIG. 4. FT-IR spectra of detonation nanodiamond particles chemical modification.

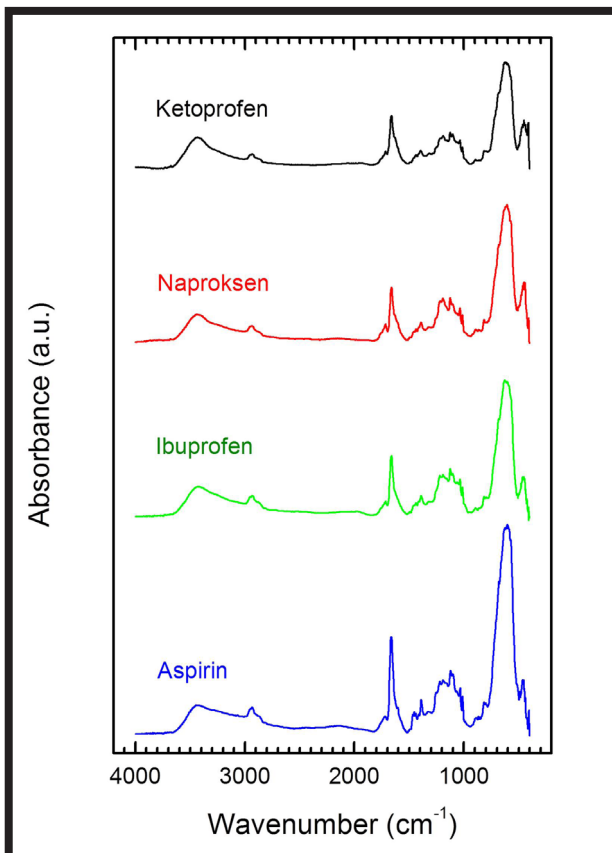


FIG. 5. FT-IR spectra of NDP with attached drugs (R-ketoprofen, R-naproxen, R-ibuprofen, R-aspirin) by ester and amine bonds and carboxyl bonds -NHCO-R.

TABLE 2. Classification of cytotoxicity of tested materials.

Tested samples	Cyto-toxicity	Reactivity
NDP-NHCO-ketoprofen	1	slight
NDP-NHCO-naproxen	1	slight
NDP-NHCO-ibuprofen	1	slight
NDP-NHCO-aspirin	1	slight
NDP-NHCO- $\beta$ -Ala-NHCO-ketoprofen	1	slight
NDP-NHCO- $\beta$ -Ala-NHCO-naproxen	1	slight
NDP-NHCO- $\beta$ -Ala-NHCO-ibuprofen	1	slight
NDP-NHCO- $\beta$ -Ala-NHCO-aspirin	1	slight

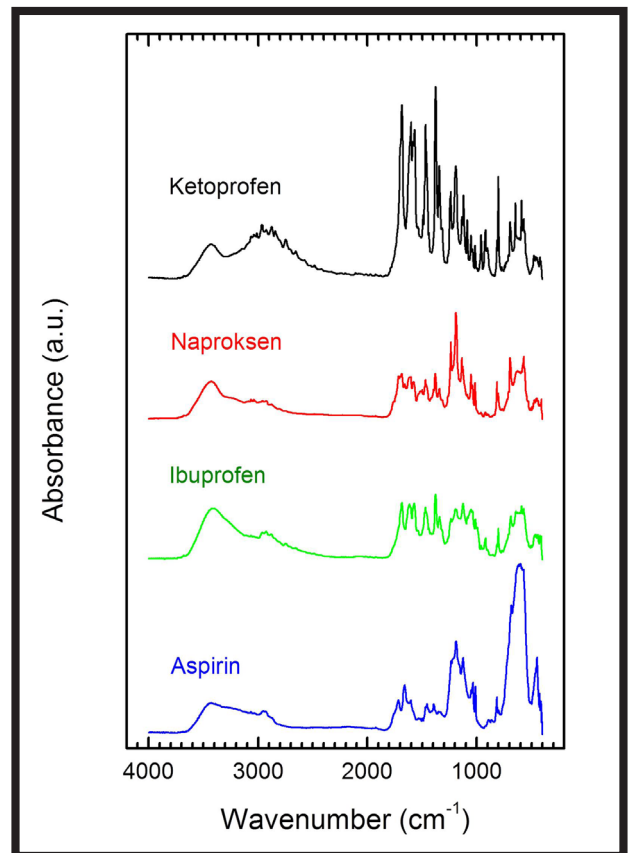


FIG. 6. FT-IR spectra of NDP with attached drugs (R-ketoprofen, R-naproxen, R-ibuprofen, R-aspirin) by amide bond with  $\beta$ -alanine connector -NHCO- $\beta$ -Ala-NHCO-R connector.

The results of in vitro examinations with mouse fibroblasts L929 (ATCC CCL-1) show the low cytotoxicity of both method of chemical modifications (TABLE 2). The comparison between the chemical modification of nanodiamond particles by anti-inflammatory drugs without and with  $\beta$ -alanine linker shows slight differences of cytotoxicity although the more biocompatible seems to be modification without  $\beta$ -alanine. Surface modification of nanodiamond particles by ibuprofen without a connector exhibits the lowest cytotoxicity to examined cell line, and aspirin exhibits the lowest cytotoxicity (the absence of necrotic cells) for nanodiamond modified with  $\beta$ -alanine (FIG. 7).

FIGs 8 and 9 show the microscopic images of cells in a direct contact cytotoxicity test. The presence of living cells in contact with the chemically modified nanodiamonds indicates green fluorescence. The obtained results show very low and not statistically significant cytotoxicity of detonation nanodiamond particles, chemically modified by non-steroidal anti-inflammatory drugs in cultures of mouse fibroblasts (FIGs 8 and 9).

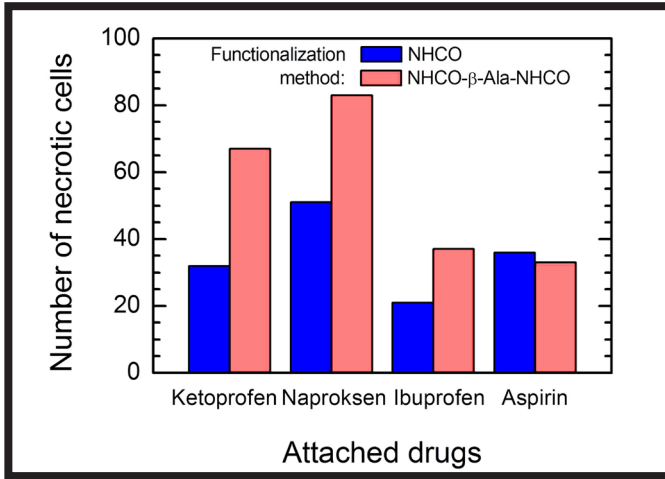


FIG. 7. Number of necrotic cells in the tested NDP samples with attached drugs (ketoprofen, naproxen, ibuprofen, aspirin) after 24 h direct cytotoxicity test for two different methods of their functionalization: "NHCO" and "NHCO-β-Ala-NHCO".

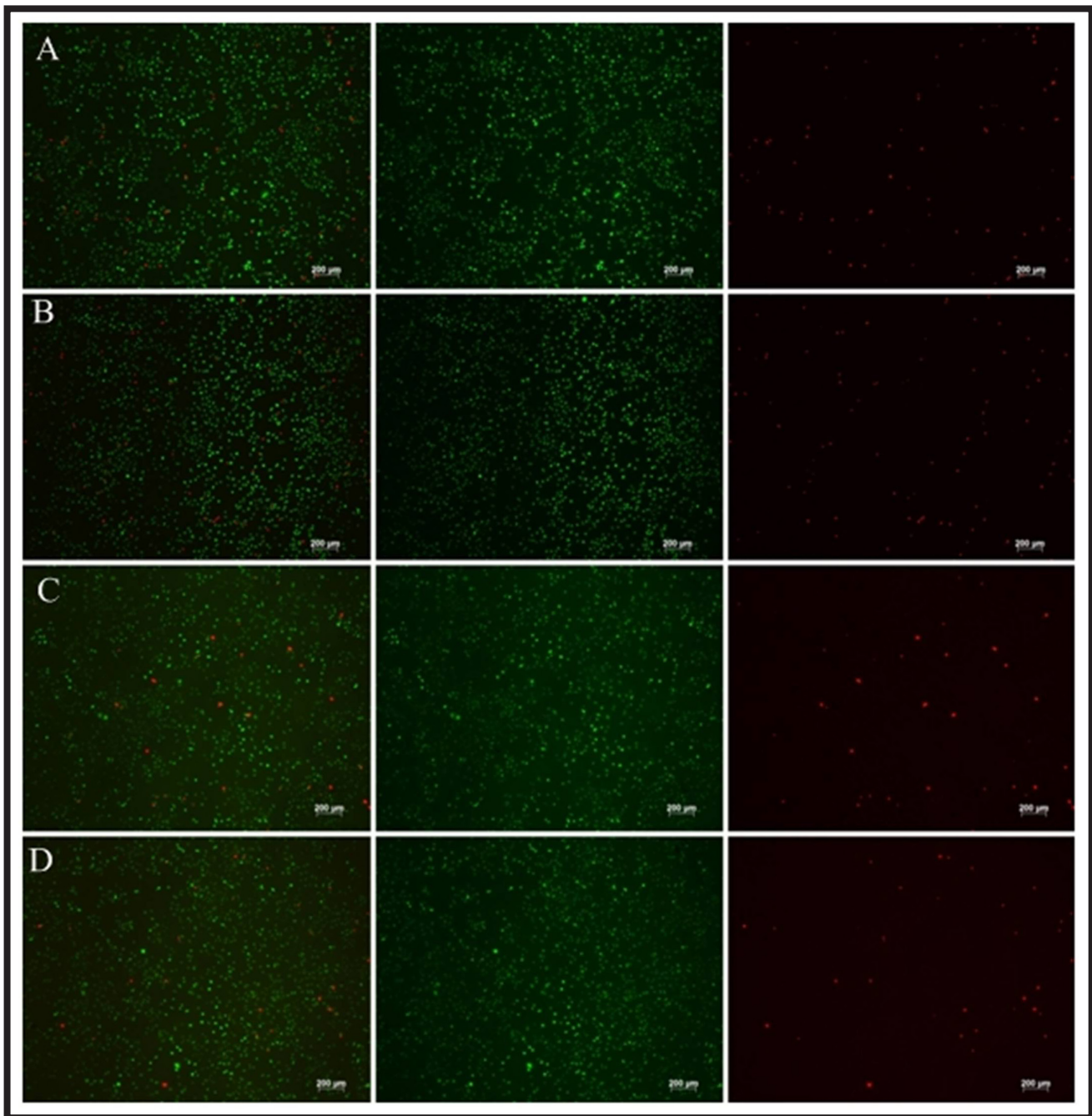
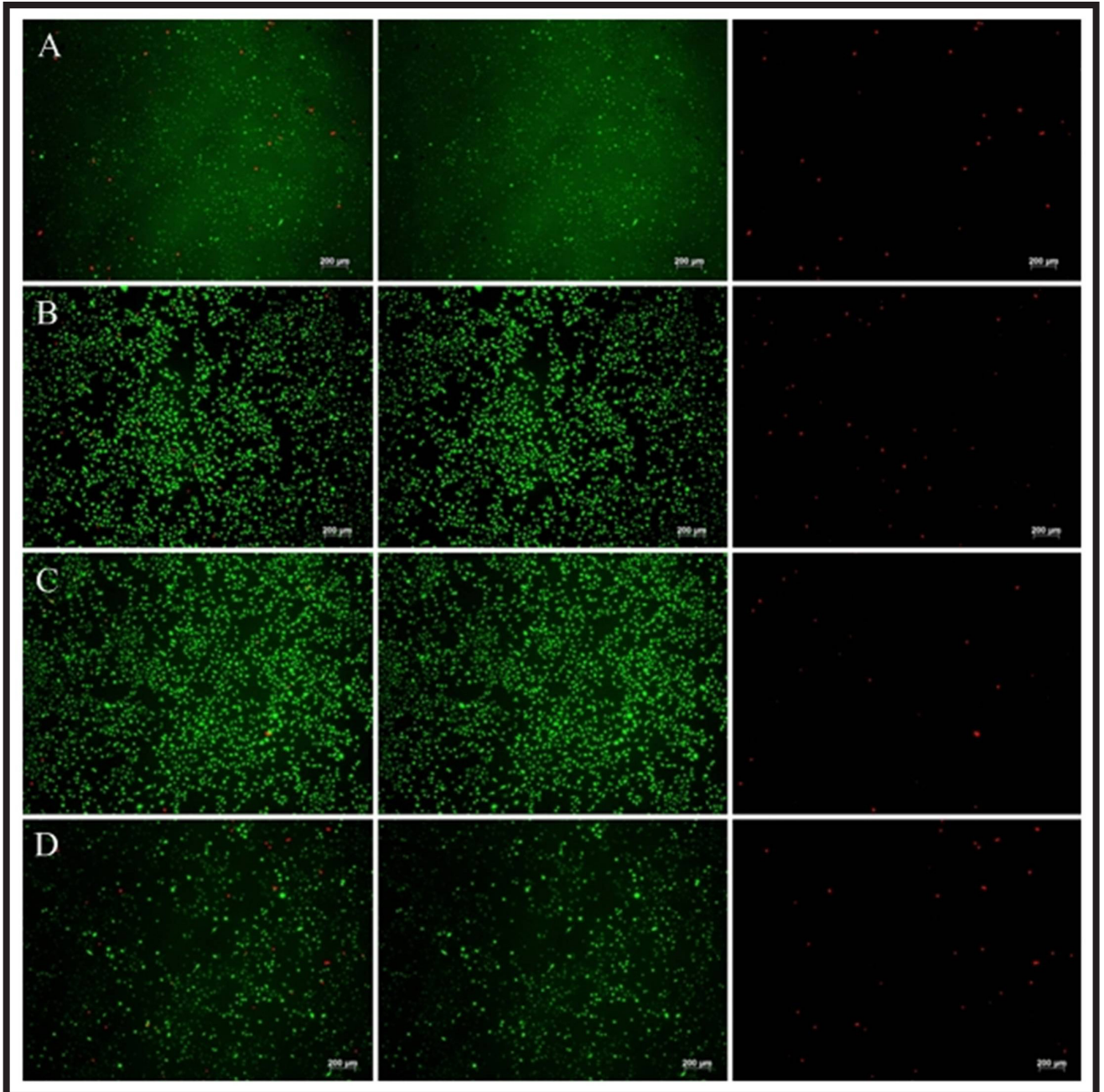


FIG. 8. Microscopic image of cells in direct contact cytotoxicity test of the following materials: A - NDP-NHCO-ketoprofen, B - NDP-NHCO-naproxen, C - NDP-NHCO-ibuprofen, D - NDP-NHCO-aspirin. Living cells positive to the FDA - green fluorescence, PI positive necrotic cells - red fluorescence, FDA + PI channel.



**FIG. 9. Microscopic image of cells in direct contact cytotoxicity test of the following materials: A - NDP-NHCO- $\beta$ -Ala-NHCO-ketoprofen, B - NDP-NHCO- $\beta$ -Ala-NHCO-naproxen, C - NDP-NHCO- $\beta$ -Ala-NHCO-ibuprofen, D - NDP-NHCO- $\beta$ -Ala-NHCO-aspirin. Living cells positive to the FDA - green fluorescence, PI positive necrotic cells - red fluorescence, FDA + PI channel.**

The number of patients with cardiovascular diseases who, due to the exhaustion of the conventional treatment opportunities, need to have the heart bioprosthesis applied constantly increases. The increasing expectations are also associated with the introduction into the clinical practice the treatment that uses the stem cells in which, apart from the proper selection of the type of the implanted cells it is very important to optimize methods for the transfer of cells into the affected area. Both, in the case of heart bioprostheses design and scaffolds for cell transfer, except for the appropriate design solutions, it is essential to use the advanced innovative biomaterials. Such materials ought to be biocompatible and should allow for proper cultivation of cells.

It is recommended that the cells after the cultivation process are characterized by high viability, the preservation of normal morphology, good growth, adhesion and migration deep into the scaffold. In the case of stem cells, it is also essential to stimulate the differentiation of the cells. Because of the increasing disparity between the number of donors and recipients, seeking for optimal materials, due to the prolonged contact with the blood, somatic and stem cells, seems to be crucial. Such materials may be based on natural biological human or zoonotic tissues; however, synthetic materials may be used as well. Both in the case of biological and synthetic materials, the normal cell interaction with the substrate is determined by the surface modification of materials.

Great hopes, due to the biological characteristics, are placed in nanodiamonds. They may stabilize, in the mechanical way, the applied surface. They may also stimulate cellular processes, particularly in the case of conjugation with the biologically active agents. Therefore, it is vital to carry out cytotoxicity test of such materials. This allows for the pre-selection of the particles for surface modification purpose. In order to do so, tests that use the model cells – fibroblasts are frequently applied. In these studies it is shown that fibroblasts in contact with the tested biomaterial particles retain their high cell viability. They also reveal proper adhesion to the substrate. This may indicate a possibility of nanodiamonds employment in applications related to the tissue engineering. The present results are very promising, however, in the future the scope of research needs to be broadened and, above all, there is a need for a strong focus on the influence of diamond powders or substrates, modified by diamond powders, on mesenchymal cells. Such studies will certainly allow for coming closer to the research model for *in vivo* applications in models of large animals and, in the future, in clinical studies.

The nanodiamond powders produced by the detonation method with a grain size of 2-5 nm display a high biological activity at the molecular level affecting the expression of genes responsible for inhibition of oxidative stress and carcinogenic processes [29-31]. The diamond phase content, the grain size and the method of obtaining carbon powders, including nanodiamonds, significantly affect their biological activity [31]. The functionalization of nanopowder surface increases the possibility of the controlled activity of the nanodiamond surface, e.g.: towards reducing the inflammatory reaction and antibacterial activity, and to create a biosensor that is sensitive to the presence of pathogenic bacteria in the presence of the nanodiamond [6].

The functionalization of nanoparticles is aiming to change and/or improve their biological properties. From the perspective of obtaining the modified nanoparticles, the approach based on the physical deposition of the modifying compound on a solid nanocarrier is easier. However, from the point of view of using the modified nanoparticles in *in vitro* tests such approach carries the risk of too rapid release of the physically related compounds. The sustainability improvement can be achieved through the use of covalent bonding methods between nanoparticles and the compounds of interest.

In this approach, also, it is possible to modulate the stability of the conjugates by selecting the nature of covalent bonds between the nanoparticle and the ligand. The amide bond, used in the research, formed between H<sub>2</sub>N-NDP and the carboxyl groups of non-steroidal anti-inflammatory drugs (aspirin, ibuprofen, ketoprofen and naproxen) should ensure the relative stability and thus, the resistance to proteolytic enzymes.

The key factor assuring success in the acylation of amine groups on the surface of the nanoparticle by acid derivative (**4a-d** respectively) is the selection of an efficient condensing agent, allowing for formation of the amide bond in the amphiphilic environment. The amphiphilicity of the environment is the result of the polar character of the amine groups on the surface of nanopowders and hydrophobic nature of the NDP. In the study, as a condensing reagent, was used a quaternary salt of N-Triazinylammonium DMT / NMM / Tos<sup>-</sup> **5**, which is an efficient condensing reagent in the synthesis of both polar and hydrophobic objects.

The structure of the triazine esters **6a-d**, which are appropriate acylating reagents, was confirmed on the basis on the IR testing, where was observed a characteristic band in the range of 1750 to 1780 cm<sup>-1</sup>. Another very important factor, regarding the modification of solid carriers, is the efficiency of the removal of reaction by-products, thereby eliminating the deposition of deposits in the functionalized material. The use of a triazine condensing reagents provides this aspect, since the 2-hydroxy-4,6-dimethoxy-1,3,5-triazine is easily removed by polar solvent or water extraction. The structure of final derivatives of non-steroidal anti-inflammatory drugs attached to the NDP surface was confirmed by the FT-IR analysis.

During the study we obtained NDP modified by non-steroidal anti-inflammatory drug (NSAID) in which an additional link between the NDP surface and the acid residue was inserted. As the connector the rest of β-alanine was used. The selection of the amino acid was not random. At first, we expected that the nature of the amino acid linker will improve the biocompatibility of conjugates, on the other hand, the introduction of β-amino acid residues provides resistance to proteolytic enzymes. The synthesis of conjugates **9a-d** included additionally the stage of incorporation of Fmoc of the blocked amino acid and its deprotection by piperidine. The final step was the acylation of the amino group with a triazine esters **6a-d**.

## Conclusions

The results of FT-IR spectroscopy proved nanodiamond's surface modification by ketoprofen, naproxen, ibuprofen and aspirin.

Mouse fibroblasts in contact with the tested detonation nanodiamond particles retain their high cell viability.

Chemically modified detonation nanodiamond particles by non-steroidal anti-inflammatory drugs reveal the low cytotoxicity towards mouse fibroblasts.

The chemical modification of detonation nanodiamond particles gives the possibility to control the surface reactivity of nanodiamonds.

Currently, it is possible to obtain the chemically functionalized nanodiamond particles containing functional groups as the linkers for bioactive molecules.

## Acknowledgements

*A financial support of this studies by grant donated by The National Centre for Research and Development, no. PBS2/A5/31/2013 is acknowledged.*

## References

- [1] Y. Xing, L. Dai: Nanodiamond in nanomedicine. *Nanomedicine* 4 (2009) 207-218.
- [2] V.V. Danilenko: On the history of the discovery of nanodiamond synthesis. *Phys. Solid. State.* 46 (2004) 595-599.
- [3] V.Yu. Dolmatov: Modern industrial technology of reception detonation nanodiamonds and the basic areas of their use. *Nanotechnics* 1 (2008) 56-78.
- [4] A. Krüger: The structure and reactivity of nanoscale diamond. *J. Mater. Chem.* 18 (2008) 1485-1792.
- [5] O.A. Shenderova, G. McGuire, *Nanocrystalline Diamond*, in: Y. Gogotsi, (Eds.), *Nanomaterials handbook*. CRC Press, Taylor and Francis Group, Boca Raton, 2006, 203-237.
- [6] K. Mitura, I. Gisterek, P. Ceynowa, A. Wachowicz, G. Pich, R. Woś, K. Adach: Badania mikrobiologiczne bioaktywnych proszków nanodiamantowych modyfikowanych chemicznie, in: L. Leniowska, Z. Nawrat, (Eds.), *Postępy inżynierii biomedycznej*, Uniwersytet Rzeszowski, Rzeszów, 2013, 157-167.
- [7] K. Adach: Chemical modification of diamond nanoparticles produced by detonation method. PhD Thesis, Technical University of Łódź, 2013.
- [8] P. Ceynowa, K. Mitura, W. Zinka, S. Mitura: System modyfikacji nanoproszków diamentowych (DPP) w rotacyjnej komorze reaktora plazmo-chemicznego (MW PACVD). *Elektronika* 10 (2014) 47-50.
- [9] Ah-Y. Jee, M. Lee: Surface functionalization and physicochemical characterization of diamond nanoparticles. *Curr. Appl. Phys.* 9 (2009) 144-147.
- [10] I. Larionova, V. Kuznetsov, A. Frolov, O. Shenderova, S. Moseenkov, I. Mazov: Properties of individual fractions of detonation nanodiamond. *Diam. Relat. Mater.* 15 (2006) 1804-1808.
- [11] O.A. Shenderova, D.M. Gruen: *Ultrananocrystalline Diamond: Synthesis, Properties, and Applications*. ed. William Andrew Publishing Norwich, New York, 2006.
- [12] O.A. Shenderova, S.A. Ciftan Hens: *Detonation Nanodiamond Particles Processing, Modification and Bioapplications*, in: D. Ho (Eds.), *NANODIAMONDS. Application in Biology and Nanoscale Medicine*, Springer, New York, 2010.
- [13] A.P. Puzyr, A.V. Baron, K.V. Purtov, E.V. Bortnikov, N.N. Skobelev, O.A. Mogilnaya, V.S. Bondar: Nanodiamonds with novel properties: A biological study. *Diam. Relat. Mater.* 16 (2007) 2124-2128.
- [14] V.N. Mochalin, O. Shenderova, D. Ho, Y. Gogotsi: The properties and applications of nanodiamonds. *Nat. Nanotechnol.* 7 (2012) 11-23.
- [15] M.V. Baidakova, Y.A. Kukushkina, A.A. Sitnikova, M.A. Yagovkina, D.A. Kirilenko, V.V. Sokolov, M.S. Shestakov, Ya.A. Vul, B. Zousman, O. Levinson: Structure of nanodiamonds prepared by laser synthesis. *Phys. Solid. State.* 55 (2013) 1747-1753.
- [16] E.V. Basiuk, A. Santamaria-Bonfil, V. Meza-Laguna, T.Y. Gromovoy, E. Alvarez-Zauco, E.F. Contreras-Torres, J. Rizo, G. Zavala, V.A. Basiuk: Solvent-free covalent functionalization of nanodiamond with amines. *Appl. Surf. Sci.* 275 (2013) 324-334.
- [17] P. Wilczek, A. Lesiak, A. Niemieć-Cyganek, B. Kubin, R. Słomski, J. Nozyski, G. Wilczek, A. Mzyk, M. Gramatyka: Biomechanical properties of hybrid heart valve prosthesis utilizing the pigs that do not express the galactose- $\alpha$ -1,3-galactose ( $\alpha$ -gal) antigen derived tissue and tissue engineering technique. *J. Mater. Sci-Mater.M.* 26 (2014) 5329.
- [18] P. Wilczek, Z. Malota, A. Baranska, A. Niemieć-Cyganek, B. Kubin, R. Słomski, J. Nozyski, G. Wilczek, A. Mzyk, M. Gramatyka, J. Opiela: Age-related changes in biomechanical properties of transgenic porcine pulmonary and aortic conduits. *Biomedical Materials. Biomed. Mater.* 9 (2014) 055006.
- [19] P. Wilczek, R. Major, L. Lipińska, J. Lackner, A. Mzyk: Thrombogenicity and biocompatibility studies of reduced graphene oxide modified acellular pulmonary valve tissue. *Mat. Sci. Eng. C-Mater.* 53 (2015) 310-321.
- [20] J.-I. Chao, E. Perevedentseva, P. Chung, K.-K. Liu, Ch.-Y. Cheng, Ch.-Ch. Chang, Ch.-L. Cheng: Nanometer-Sized Diamond Particle as a Probe for Biolabeling. *Biophys. J.* 93 (2007) 2199-2208.
- [21] T.-J. Wu, Y.-K. Tzeng, W.-W. Chang, Ch.-A. Cheng, Y. Kuo, Ch.-H. Chien, H.-Ch. Chang, J. Yu: Tracking the engraftment and regenerative capabilities of transplanted lung stem cells using fluorescent nanodiamonds. *Nat. Nanotechnol.* 8 (2013) 682-689.
- [22] T. Bursleson, N. Yusuf, A. Stanishevsky: Surface modification of nanodiamonds for biomedical application and analysis by infrared spectroscopy. *JAMME.* 37 (2009) 258-263.
- [23] R.J. Edgington, A. Thalhammer, J.O. Welch, A. Bongrain, P. Bergonzo, E. Scorsone, R.B. Jackman, R. Schoepfer: Patterned neuronal networks using nanodiamonds and the effect of varying nanodiamond properties on neuronal adhesion and outgrowth. *J. Neura. Eng.* 10 (2013) 056022.
- [24] E. Marianne, J. Mertens, J. Frese, D. A. Bölükbas, L. Hrdlicka, S. Golombek, S. Koch, P. Mela, S. Jockenhövel, F. Kiessling, T. Lammers, FMN-Coated Fluorescent USPIO for Cell Labeling and Non-Invasive MR Imaging in Tissue Engineering. *Theranostics.* 4 (2014) 1-10.
- [25] R. Martin, P. Heydron, M. Alvaro, H. Garcia: General Strategy for High-Density Covalent Functionalization of Diamond Nanoparticles Using Fenton Chemistry. *Chem. Mater.* 21 (2009) 4505-4514.
- [26] M. Satyanarayana, F. Vitali, J.R. Frost, R. Fasan: Diverse organo-peptide macrocycles via a fast and catalyst-free oxime/intermediate-mediated dual ligation. *Chem. Commun.* 48 (2012) 1461-1463.
- [27] B. Kolesinska, K.K. Rozniakowski, J. Fraczyk, I. Relich, A.M. Papini, Z. Kamiński: The Effect of Counterion and Tertiary Amine on the Efficiency of N-Triazinylammonium Sulfonates in Solution and Solid-Phase Peptide Synthesis. *J. Eur. J. Org. Chem.*, doi.org/10.1002/ejoc.201402862, 2 (2015) 401-408.
- [28] K.G. Jastrzabek, R. Subiros-Funosas, F. Albericio, B. Kolesinska, Z. Kaminski: 4-(4,6-Di[2,2,2-trifluoroethoxy]-1,3,5-triazin-2-yl)-4-methylmorpholinium Tetrafluoroborate. Triazine-Based Coupling Reagents Designed for Coupling Sterically Hindered Substrates. *J. Org. Chem.* 76 (2011) 4506-4513.
- [29] K. Bakowicz-Mitura, G. Bartosz, S. Mitura: Influence of diamond powder particles on human gene expression. *Surface and Coatings Technology* 201 (2007) 6131-6135.
- [30] T. Niemieć, M. Szmiedt, E. Sawosz, M. Grodzik, K. Mitura: The effect of diamonds nanoparticles on redox and immune parameters in rats. *Journal of Nanoscience and Nanotechnology* 11 (2011) 1-6.
- [31] M. Czerniak-Reczulska, P. Niedzielski, A. Balcerczyk, G. Bartosz, A. Karowicz-Bilinska, K. Mitura: Biological properties of different type carbon particles in vitro study on primary culture of endothelial cells. *Journal of Nanoscience and Nanotechnology* 10 (2010) 1065.

# INTERACTIONS OF CARBON NANOPARTICLES FROM PACKAGINGS WITH COMPONENTS OF FOOD, DRUGS AND BIOLOGICALLY ACTIVE MOLECULES - A REVIEW

JOLANTA WRÓBLEWSKA-KREPSZTUL<sup>1</sup>, IWONA MICHALSKA-POŻOGA<sup>1</sup>, MIECZYSLAW SZCZYPIŃSKI<sup>1</sup>, PIOTR WILCZEK<sup>2</sup>, TOMASZ RYDZKOWSKI<sup>3\*</sup>

<sup>1</sup> PK KOSZALIN UNIVERSITY OF TECHNOLOGY, DEPARTMENT OF MECHANICAL ENGINEERING, RACŁAWICKA 15-17, 75-620 KOSZALIN, POLAND

<sup>2</sup> HEART PROSTHESIS INSTITUTE OF THE FOUNDATION OF CARDIAC SURGERY DEVELOPMENT, WOLNOSCI 345A, 41-800 ZABRZE, POLAND

<sup>3</sup> UWM UNIVERSITY OF WARMIA AND MAZURY IN OLSZTYN, FACULTY OF TECHNICAL SCIENCES, OCZAPOWSKIEGO 11, 10-719 OLSZTYN, POLAND

\* E-MAIL: TOMASZ.RYDZKOWSKI@TU.KOSZALIN.PL

## Abstract

*Nanomaterials are very important in the field of packaging of food, medicines and dietary supplements. Modern packagings often contain nanoparticles that provide them new feature - nanoparticles are used to activate mainly the packaging inner surface. Carbon occurs in several allotropic forms, such as diamond, graphite (including nanotubes and fullerenes), carbides, and nanocrystalline diamond which is produced in a process of radio frequency plasma activated chemical vapor deposition (RF PA CVD). Variety of allotropic forms of carbon results in different chemical and biological interactions between carbon nanoparticles and the polymer matrix material. Carbon nanoparticles can be used to activate the inner surface of packagings. There is a growing demand for food free of harmful chemicals such as chloramphenicol or toxic food colorings (metanil yellow, auramine, orange II or red aura). The use of nanotechnology in the food packaging sector opens up new possibilities for creating sensors to detect certain harmful analytes. These sensors are easy and quick to use. The basis of their actions is to understand the interactions between nanoparticles and chemicals. Nanoparticles can be utilized to create intelligent high performance packaging materials for contact with food, drugs and biologically active molecules, which will be safe for health of the consumers.*

**Keywords:** interaction, carbon, nanopracticles

[*Engineering of Biomaterials* 140 (2017) 21-27]

This article was presented at 10<sup>th</sup> International Forum on Innovative Technologies for Medicine – ITMED, 7-9 November 2016, Warsaw, Poland.

## Introduction

Food can be called “nanofood” when nanoparticles, nanotechnology tools or techniques are used during its production, cultivation, packaging or processing. This does not mean that food is modified at atomic level or is produced by nanomachines. Strategies to apply nanoscience to the food industry are quite different from traditional applications of nanotechnology [1,2]. This is why the definition of food control and functional food is changing.

“Nano” approach can be used to control and manipulate interactions between food ingredients such as proteins, lipids and polysaccharides providing desirable rheological and structural properties of food [2,3].

There are several advantages of materials in the form of nanoscale objects in comparison with micro scale objects. Nanoscale materials act in a different way than typical macroscale materials [2,4]. Recently, innovations in packaging industry turn from the macroscopic to the nano-scale. It really becomes important to develop food products using nanomaterials, chemical and physical properties. Nanotechnology and nanosciences should be used together in food innovations, novel food development, dietary supplements as well as medicines and biologically active molecules [2,3].

This review paper presents recent advances in application of carbon nanoforms in the packaging of food, dietary supplements, drugs and biologically active molecules.

### Nanocomposites consisting of carbon nanotubes for the detection of toxic substances in food and dietary supplements

Growing concerns about the safety and security of food, cause that cheaper and faster methods of contaminants detecting are developing to ensure safety of food [5-7]. Chloramphenicol is a well-known veterinary medicine with a broad spectrum of activity for the treatment of infectious diseases in animals [7-9]. Chloramphenicol overdose leads to chronic toxicity resulting in myelosuppression and aplastic anemia [7,10,11]. The use of chloramphenicol in poultry, aquatic and other animals for food production was banned by the United States, European Union, Canada and China [12]. Therefore, the development of sensitive and rapid methods for monitoring of chloramphenicol in food samples is crucial to maintaining food safety. Reports in the literature describe the electrochemical method of detecting low levels of chloramphenicol to 15 nM. Detection is possible through a combination of molybdenum sulfide and multiwalled carbon nanotubes (MWCNTs) - FIG. 1. Detection of this substance is possible in real samples such as milk, powdered milk or honey. The advantages of this method are: simple and ecological process of preparation, fast analysis time, good reproducibility. Negatively charged multiwalled carbon nanotubes are mixed with particles of molybdenum sulfide, forming a grid on the 3D structure. The hierarchical structure of the 3D nanocomposite constructed of molybdenum sulfide and functionalized multiwalled carbon nanotubes (f-MWCNTs) significantly increases synergistic affinity for chloramphenicol. The sensor operates in a wide linear range from 0.08 to 1392 IM. The detection limit is 0.015 IM ±0.003 and exceeds the limits of detection of the previously modified electrodes. Scientists want to target their work towards miniaturization of electrodes for the rapid detection of chloramphenicol in samples on the spot. Combination of nanocomposite molybdenum sulfide and multiwalled carbon nanotubes is highly promising in the analysis of food safety, medicines and dietary supplements [7].

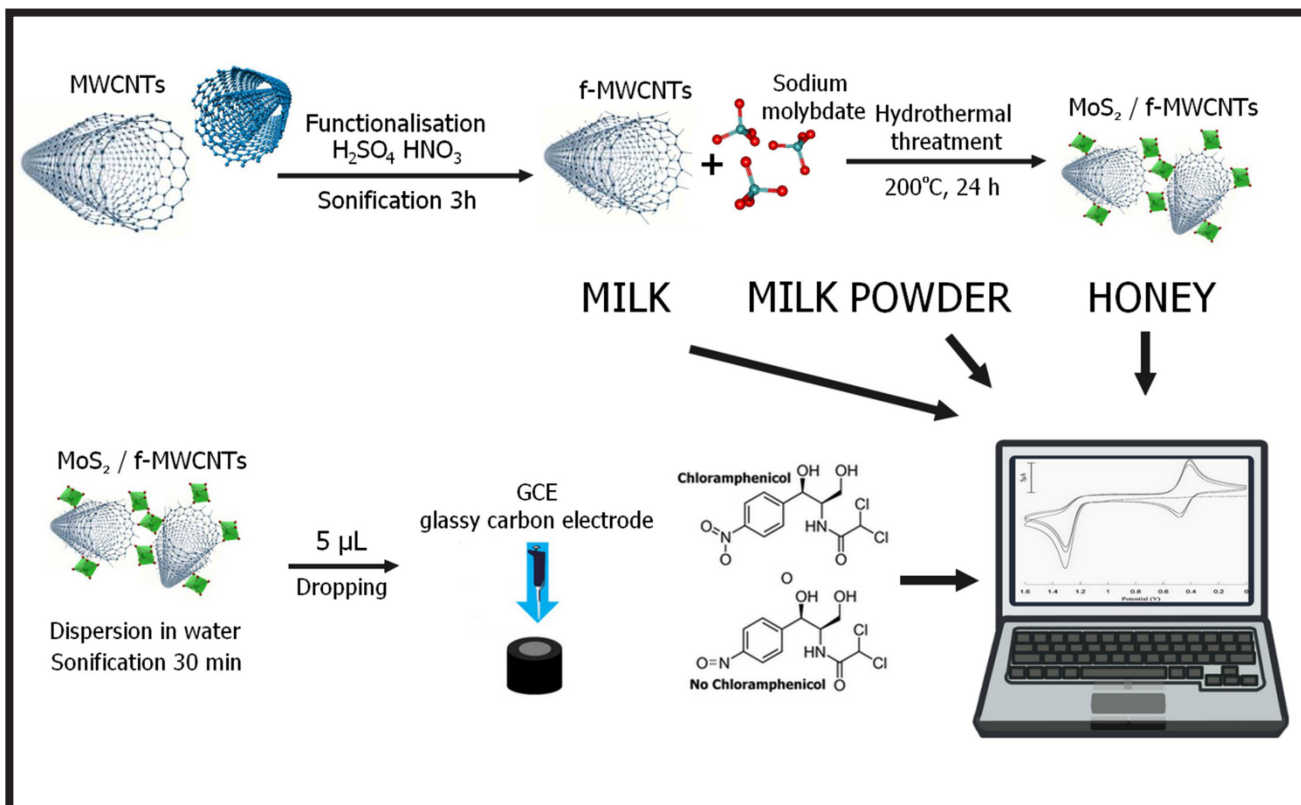


**FIG. 1.** Determination of chloramphenicol using nanocomposite molybdenum sulfide/multiwalled carbon nanotubes  $\text{MoS}_2/\text{f-MWCNTs}$ , food, and biological and pharmaceutical samples. Developed on the basis of [7].

In the case of food, besides microbiological control it is very important to monitor false, toxic food dyes. This is important because of their potential toxicity and virulence. A hybrid composite, which can be regarded as a sensor for rapid detection of toxic dyes such as metanil yellow, auramine, orange II and aura red has been developed. The hybrid nanocomposite was made with onions nanocarbon-polyoxometalate. The composite allows the detection of trace amounts of toxic dyes used in food, beverages, syrups, and drugs. The water-soluble polyoxometalates belong to the family of anionic metals inorganic oxide, a complex that can be synthesized by simple chemical processes with water [13,14]. This connection allows to identify the toxic chemicals in the smallest amount and can be used in detecting trace amount of toxic dyes (Auramin O and Orange II) used in food. Auramin O is a carcinogen which damages human eye and causes DNA damage. Orange II is toxic azo dye, commonly used in organic light emitting and it affects blood cell. Metanil yellow is used to check the behavior of the composite (FIG. 2). The observation and study of the interaction of carbon nanoparticles with biological material and chemicals gives great possibilities of limiting the amount of toxic substances in food. Hybrid of carbon nano-onion with polyoxometalate nanoparticles may combine the properties of two ideal functional nanomaterials to get a wide range of applications which will accelerate the development of nanoscience and nanotechnology.

The lanthanide polyoxometalate / carbon nano-onion composites have fluorescence properties. In the presence of  $1.71 \times 10^{-5}$  lanthanide-polyoxometalate cluster with different concentration of aqueous solution of metanil yellow, no change in intensity of yellow color was observed; on the other hand in the presence of  $3.43 \times 10^{-6}$  mol/ml<sup>-1</sup> carbon nano-onion, there was a change in intensity but that was in the micro range ( $1.03 \times 10^{-2}$  µmol /ml<sup>-1</sup>) [14]. FIG. 3 shows change in fluorescence intensity based on varied concentration of the food color with fixed concentration of  $[\text{Na}_{10}(\text{PrW}_{10}\text{O}_{36})_2 \cdot 130\text{H}_2\text{O}/\text{CNO}]$  nanocomposite [14].

Polydiacetylene (PDA) is a self-assembled polymer with a closely packed and well-aligned conjugated backbone [15-17]. Polydiacetylene monomers in aqueous solution form nano-sized vesicles. To assure specificity to the target analyte vesicle polydiacetylene surfaces are functionalized using a specific probe [17, 18]. After binding polydiacetylene vesicle to the target analyte change in color from blue to red due to the physical stress induced by the interaction between the immobilized probe and the analyte is observed. Color of polydiacetylene vesicle indicates the presence of the target analyte. Its concentration can be calculated by determining the degree of color transition [17, 19]. The sensors are attractive because the detection of the target analyte is simple. However, the disadvantage is that color change of vesicle polydiacetylene is not enough if the concentration of analyte is too low. It is thus possible to detect the analyte if its concentration is high [17].

Silver nanoparticles formed on the surface of graphene by reduction, can be used to detect different dyes. Experimental results indicate that the silver nanoparticles with graphene can identify different colorants, due to the strong interactions between graphene and dye adsorbed [17].

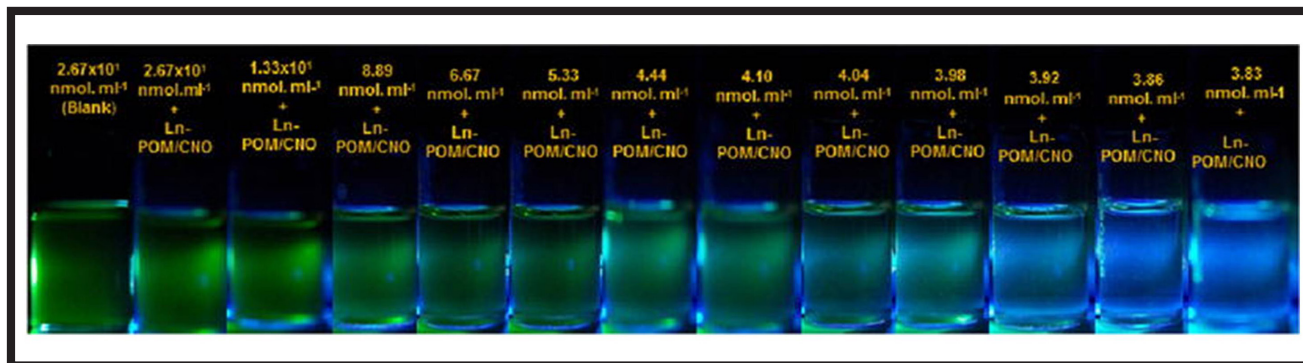


FIG. 2. Changes in fluorescence of different concentration of metanil yellow in  $3.43 \times 10^{-6} \text{ mol/ml}^{-1}$  aqueous solution of the Ln-POM/CNO nanocomposite (lanthanide polyoxometalate/carbon nano-onion). Reprinted with Creative Commons Attribution 4.0 International License permission from [14].

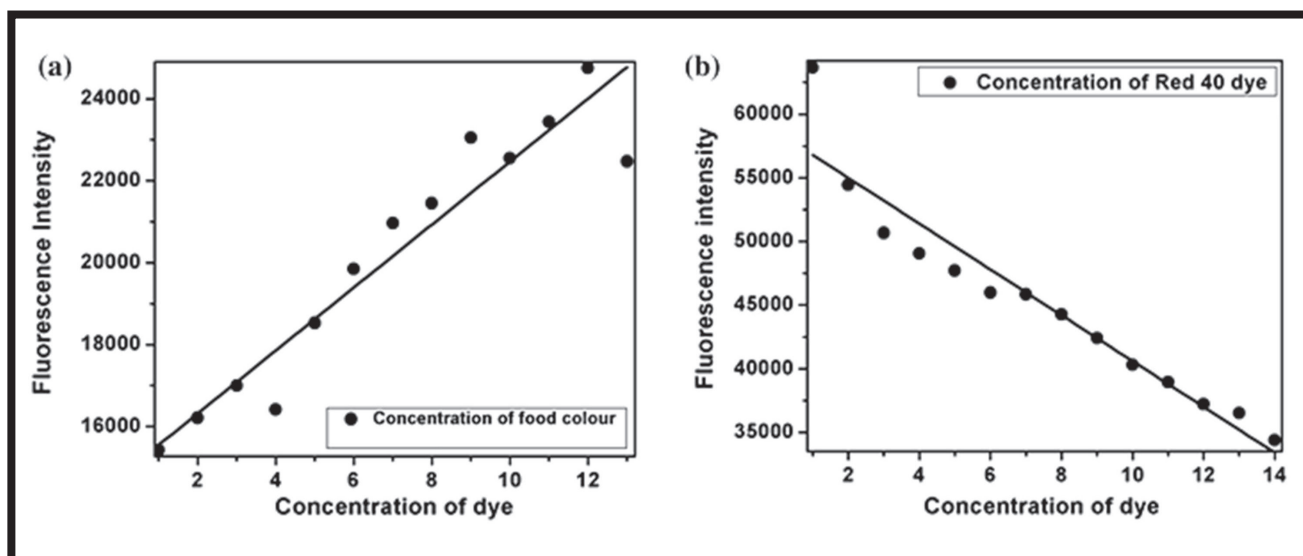


FIG. 3. a) Change in fluorescence intensity of metanil yellow dye (similar behavior for auramine O and orange II food color, data not shown); b) Change in fluorescence intensity for red 40 dye. Reprinted with Creative Commons Attribution 4.0 International License permission from [14].

### Nanoparticles in materials that come into contact with food, dietary supplements and biologically active substances

Melamine (1,3,5-triazine - 2,4,6-triamine) is an industrial chemical often used in the production of melamine formaldehyde resins and plastics for coating, commercial filters or laminates. It is a chemical industrial raw material used in the food technology [21,22]. Some of the products such as melamine tableware were used in the catering industry and have become an important material for food contact. Melamine has a high level of nitrogen by weight - 66%, is of low cost, and began to be illegally used in food, in particular milk products, for the creation of the apparent protein content [22,23]. Melamine itself has low toxicity, but in the body it tends to form insoluble melamine crystals in the kidneys, can cause damage of the kidneys and the urinary tract, and even can lead to death [22,24]. Melamine can migrate in food and cause health risks [22,23]. To ensure food safety and protect human health the migration of monomers from a material that is in contact with food has been strictly regulated in many countries.

Based on the European Union regulation on plastics intended to come into contact with foodstuffs (European Union 10/2011), melamine is subject to specific migration limit of  $2.5 \text{ mg} \cdot \text{kg}^{-1}$ . In view of the proven toxicity of mela-

mine United States Food and Drug Administration (FDA) has established safety limit intake of this substance in an amount of  $2.5 \text{ ng mL}^{-1}$  for adults, and  $1 \text{ g of food mL}^{-1}$  of an infant formula [22,25].

Literature describes various methods for determination of melamine such as capillary electrophoresis, high performance liquid chromatography, gas chromatography mass spectrometry, fluorescence, colorimetric method, surface enhanced Raman scattering, electrochemical techniques [22,26-33].

Graphene is a single-layer and two-dimensional material whose properties like rapid electronic transfer and high surface area make it an ideal material for electrochemistry [22,34].

For designing of chemical sensors functionalization of graphene with metallic nanoparticles such as gold, platinum or palladium is used. In particular promising application is to create nanocomposites composed of graphene nanoparticles and gold. Such a combination has been used as the matrix electrodes for amperometric detection or determination of dopamine hydroquinone and catechol [22,35,36]. Gold nanoparticles/reduced graphene oxide (rGO) nanocomposites were synthesized by in situ growth Au nanoparticles on the surface of graphene oxide in the presence of sodium citrate and then reduced by hydrazine.

The obtained Au nanoparticles/reduced graphene oxide nanocomposites were modified on glassy carbon electrode for melamine measurement using hexacyanoferrate as electrochemical reporter. Melamine can be grafted on the surface of the Au nanoparticles by the interaction between the amino groups of the melamine and Au nanoparticles via Au-N bond, which leads to suppression of the peak current of hexacyanoferrate due to poor electrochemical activity of melamine. The degree of suppression is related to the concentration of melamine and can be used for the quantitative determination. In this electrochemical detection system graphene oxide provides a platform for uniform distribution of Au nanoparticles and increases the rate of electron transfer and the sensitivity of this method is higher.

#### Mechanisms for recognition of nanomaterials by biologically functionalized bacteria that may be relevant in the pharmaceutical industry

The basis of nano biorecognition is a coupling of biomolecular nanomaterials. It is assumed that each nanoparticle having a diameter of about 100 nm can efficiently conjugate 150-200 antibody molecules resulting in more than 300 active sites [37]. Interaction of biomolecules with nanoparticles allows creation of contacts between nanomaterials and target cells (FIG. 4). Functionalized nanomaterials are characterized by higher binding affinity than the free molecule [38]. It was shown that the affinity of the binding constant of an antibody-nanoparticle was eight times higher than the affinity of the free antibody [39]. There is a variety of surface modification strategies of nanomaterials. Generally they can be divided into direct and indirect strategies. In the case of direct strategies, biological molecules can be combined with nanoparticles by physical adsorption or covalent binding. It is recognized that the hydrophobic and electrostatic interactions are the most likely mechanisms involved in the adsorption of proteins. The surface of nanomaterials can be modified by covalent bonding of functional groups: sulfide, amine and carboxyl [40]. In the indirect method biomolecules engage nanoparticles by the bridges characterized by high affinity to each other. An example might be the interaction of biotin and avidin. Nanomaterials covered with avidin may interact with biotinylated molecules, and the process is based on the strong affinity of avidin to biotin. Modified antibiotics are also used in the selective isolation of pathogenic Gram-positive bacteria [39]. Vancomycin – a glycopeptide antibiotic – is used to identify Gram-positive bacteria by binding to a peptide (D-Ala-D-Ala) on the cell wall by hydrogen bonding [41,42].

Above interactions can be detected by electrochemical impedance [43], fluorescent microscopy [44-46], immunoassay [47-49] and confocal microscopy [50,39]. This type of research shows how chemical groups can interact and what affects the most important interactions of biological material that in the future can be very important in the development of the food industry, medicines and dietary supplements [51].

Reports in the literature describe the effect of resveratrol in the core of biopolymeric nanoparticles and its impact on the antioxidant and antitumor properties. Resveratrol is a naturally occurring polyphenolic phytoalexin produced by a number of different plants, such as grape, berry, mulberry, cranberry, peanuts [52,53]. Recently the positive impact of resveratrol on human health, such as an antioxidant, was highlighted [54].

Despite such benefits it is very difficult to use resveratrol in pharmacy as a supplement or as a functional food product due to its weak solubility in water and chemical instability and low bioavailability [53,55,56].

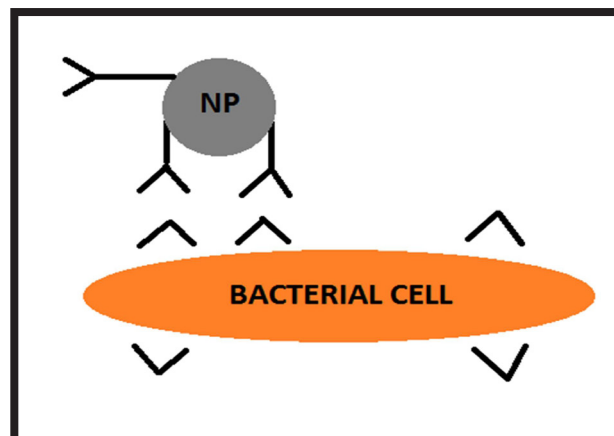


FIG. 4. Nanomaterials coated with an antibody conjugated to a bacterial cell. Developed on the basis of [39].

#### The interaction of polymer nanoparticles with cell membrane

Knowledge of the influence of the structure of nanoparticles and their interaction with cell membranes is important for understanding the effects of nano-toxicity to human and animal health and the environment and to optimize formation of nanoparticles for biomedical applications. Reports in the literature describe the interaction of the nanoparticles with the polymer of 1-palmitoyl-2-oleoyl-sn-glycero-3-phosphocholine lipid cell membranes [57]. In addition, alignment of chain segments from the polymers with that of hydrocarbon chains in the interior of the membrane facilitates the complete immersion of the nanoparticles into the cell membrane. These results highlight the importance of knowledge of the topology of the surface and structure of the polymer molecules that influence adsorption on the membrane and subsequently, induce the possible transport into the cell [57]. Effect of nanoparticles on a cell is significant, because the penetration into the cell may result in toxic effects. This can be done by endocytosis, a direct diffusion or breaking of the membrane. It is very important to construct nanoparticles with a surface morphology that does not evoke harmful effects on living organisms and at the same time would fulfil their function. Evaluation of toxicity of nanomaterials is still difficult to determine in living organisms due to the limitations of experimental techniques [57,58]. There are several factors that affect adhesion of nanoparticles to the cell membrane such as particle size, surface structure and chemical composition. Polyethylene and polystyrene are produced in huge quantities annually and are used in abundance in industry, as well as found in the environment. Simulations were based on a coarse-grain models in order to examine the trend how polystyrene nanoparticles penetrate cell membranes. The polymer particles smaller than the thickness of the membrane can more easily penetrate to hydrocarbon interior of the lipid bilayers [57,59].

Some studies have shown that the absorption of polystyrene nanoparticles inside the cell membrane might change its mechanical and structural properties. It has been shown that irreversible adhesion can be initiated by introducing the free side groups of the hydrophobic polymer in the interior of the membrane [57].

In addition, the side groups, as well as the nature of chain entanglements, can also influence the interaction with the membrane and subsequent uptake of the nanoparticles [57]. The cell membrane 1-palmitoyl-2-oleoyl-sn-glycero-3-phosphocholine is a phospholipid and composed of a polar hydrophilic phosphate heads and two hydrophobic hydrocarbon tails. The plasma membrane consists of two layers, wherein the molecules of 1-palmitoyl-2-oleoyl-sn-glycero-3-phosphocholine are arranged so that the interior of the hydrocarbon tails form the membrane and the polar main groups form a surface exposed to an aqueous medium. The polar head groups are highly soluble and can prevent polymer nanoparticles being absorbed into the more favorable hydrophobic region. However, the dangling end of the chain can readily pass through the hydrophilic barrier and be irreversibly adsorbed in contact with the upper part of the membrane of hydrocarbon chain of 1-palmitoyl-2-oleoyl-sn-glycero-3-phosphocholine. Cell membranes comprise other molecules such as sterols and proteins having different functions in the membrane. Presumably presence of all of these biomolecules can play the role in influencing the interaction of the nanoparticles with cell membranes [57].

### Carbon nanotubes and polymers

Surfactants with amphiphilic nature are extremely attractive for nanotube dispersions. There are two mechanisms of nanotube dispersion in polymers: non-wrapping and wrapping. These two mechanisms differ in the strength of adsorption between the nanotube and the polymer. Wrapping occurs when a strong single polymer layer helically wraps nanotube [60]. This is considered a very strong interaction, because it affects the electrical properties of nanotubes. In non-wrapping interaction polymers - nanotube is low due to van der Waals forces. Electrical properties are not changed in the latter case. Atomic force microscopy (AFM) observations showed that presence of polymer layers (polyvinylpyrrolidone, polystyrene) on the surface of the nanotube [61].

In 2008 Maity et al. showed that the wrapping is actually possible by the use of poly-N-vinylcarbazole (PNVC) and they produced nanocomposite of single walled carbon nanotubes and multiwalled carbon nanotubes. Monomers of poly-N-vinylcarbazole contain two aromatic rings and give a strong affinity to the surface of the nanotubes in a similar way as surfactants. The authors assessed the interaction between the nanotubes and the polymer with a Raman spectroscopy [62].

In 2003, Zheng et al. found that polythymine (T) wrapping was an enthalpically driven spontaneous process with energies favoring the interaction of polymer-nanotube instead of nanotube-nanotube binding. Using modeling, the adsorption mechanism was again thought to originate from  $\pi$ - $\pi$  interactions between the nanotube and the nucleic acid, which was further promoted by the extreme solubility of the phosphate backbone in the aqueous solution [63]. In 2005 Dror et al. described two different polymers: Gum Arabic (GA) and alternating copolymer of styrene and sodium maleate (PSSSty) to disperse nanotubes. In addition to both being amphiphilic and charged, the latter provides electrostatic repulsion, the polymers differed in two ways. GA is a highly branched polysaccharide while PSSSty is a linear copolymer of alternating hydrophobic and hydrophilic units [64]. In its aggregated state, nanotubes are not as electrically or thermally conductive and cannot provide mechanical support due to low percolation. To solve this problem, there are two chemical approaches to modifying nanotubes to make them more homogeneously dispersed in solution: covalent and non-covalent modifications. Covalent modifications involve

attaching different functional groups to the surface of nanotubes, however, these processes typically involve harsh treatments with acids as the initial step can lead to destruction of the nanotube's structure and therefore deteriorate nanotube's properties [60]. Non-covalent modifications include the use of amphiphatic molecules such as surfactants or polymers for coating the nanotubes, which stabilize the environment around them. This strategy allows to keep many important properties of nanotubes. To this end, various types of surfactants (anionic, cationic, ionic), and the polymers and their ability to spread have been tested. Recently, researchers attempt to combine these two types of molecules together in a dispersion of nanotubes [60].

### Modification of the surface of carbon nanotubes and their interactions with organic pollutants

Carbon nanoparticles have unique properties and potential for different applications. Surface properties of carbon nanoparticles affect the interaction of organic pollutants. The decreased diameter of carbon nanotubes results in increased surface area and leads to enhanced adsorption of pyrene, ofloxacin (OFL) and norfloxacin (NOR) [60,65,66].

Availability of surface to absorb contaminants on single walled carbon nanotubes could be higher than that of activated carbon with the relative effect of blocking the pores. For flat structural molecules such as benzene, flat surface makes more contact with the carbon nanotubes, so adsorption is improved with increasing diameter of nanotubes [60,67]. Adsorption is also influenced by other factors such as molecular structure, functional groups and morphology of carbon nanoparticles. Functional groups such as -OH, -COOH, and -C=O from carbon nanoparticles may be intentionally created by the method of oxidation [60,68].

The functional groups of the carbon nanoparticles can interact with water by hydrogen bonding leading to the formation of water clusters, which reduce the availability of carbon nanoparticles to interact with the surface of the organic impurities [60,69]. Increased interaction leads to the formation of bonds between functionalized carbon nanoparticles and organic pollutants. Multiwalled carbon nanotubes with -OH groups and multiwalled carbon nanotubes with -COOH groups may form a hydrogen bond with the 2-phenylphenol and enhance its adsorption [60,70]. The increase in adsorption of organic impurities is affected by the grafting of functional groups on the surface of carbon nanotubes. The adsorption capacity can be increased by adsorption of  $\beta$ -cyclodextrin on the surface of the carbon nanotubes. Such carbon nanotubes have a higher affinity for Pb (II) and 1-naphthol because hydroxyl groups and internal hydrophobic core in the cavity  $\beta$ -cyclodextrin can form complexes with metal ions and organic contaminants [60,71]. The main interactions between organic contaminants and carbon nanoparticles are hydrophobic, electrostatic, hydrogen bond, and  $\pi$ - $\pi$  interactions. These interactions and their strength are influenced by the surface properties and morphology of carbon nanoparticles and the molecular size, structures, and functional groups of organic contaminants. For a given carbon nanoparticles, various mechanisms may simultaneously control the sorption progress of organic contaminants on carbon nanoparticles, while the sorption controlling mechanisms may depend on different environmental conditions. Effects and comparison of adsorption of various organic pollutants on the carbon nanoparticles may provide important information on the relationship and the different mechanisms of action. Research should be directed toward the assessment of the dispersibility of carbon nanoparticles in a variety of environmental conditions on the characteristics of sorption of organic pollutants [60].

## Promising intelligent packagings in the food and pharmaceutical industries

The biopharmaceutical industry is developing rapidly, but every innovation must be safe. Many companies are working to develop packages that will warn of contamination of packaged food and respond to changes in environmental conditions. There are examples of nanotechnology application in the food, medical and pharmaceutical industries; this is realised by the use of nanocapsules with flavor enhancers and the nanoparticles having the ability to bind and remove chemicals from the food [72]. Intelligent packaging is a promising application of nanotechnology innovation to develop antimicrobial packaging applicable in the medical and pharmaceutical industries. Intelligent packaging can respond to the environmental conditions or warn the consumer about the contamination and the presence of pathogens. Researchers are trying to develop a package that could in time evolve preservatives to extend the shelf-life of the food product. These solutions are most exciting innovation in the food industry worldwide. Nanocrystals embedded in the plastic material help to form a molecular barrier to prevent oxygen transport. The current technique allows to preserve the freshness of the beer for 6 months and some companies are working on extending the freshness of it by using this technology for 18 months. Coatings with nanoparticles could create a kind of sensor to detect pathogens in food. Such a sensor would detect the presence of pathogens by changing the color of the packaging to alert consumers that food has become contaminated or food began to spoil. Nanosize natural biopolymers such as polysaccharides can be used to encapsulate vitamins, prebiotics and probiotics. In the food industry one of the major problems is time-consuming and laborious process of food quality control analysis. Innovative devices and techniques can be developed to facilitate the preparation of food samples for analysis. From this point of view, the development of nanosensors for the detection of microorganisms and impurities can be used in food and pharmaceutical industry [72].

## Conclusion

Nanotechnology and nanosciences have great potential for use in the food, chemical, medical and pharmaceutical industries. This gives an opportunity to raise awareness of the mechanisms of action of nanoparticles with food ingredients and drugs, as well as packaging of food and dietary supplements. Nanoparticles as active packaging components can be used for antimicrobial agents encapsulation, adsorption and chemical conjugation.

## Acknowledgements

*The work has been supported with the statutory research of Faculty of Mechanical Engineering at Koszalin University of Technology.*

## References

- [1] Ozimek L., Pospiech E., Narine S.: Nanotechnologies in food and meat processing. *Acta Sci Pol Technol Alimen* 9 (2010) 401-412.
- [2] Otles S., Yalcin B.: Food Chemistry and Nanoscience. *Journal of Nanomaterials & Molecular Nanotechnology* (2013) 2:4
- [3] Sanguansri P., Augustin M.A.: Nanoscale materials development - a food industry perspective. *Trends Food Sci Technol.* 17 (2006) 547-556.
- [4] Bugusu B.A., Bryant C.M.: Food Nanoscience in the United States and the Role of IFT, Institute of Food Technologists WAFDO Annual Conference, Denver, CO, 2007 Institute of Food Technologists.
- [5] Göğüs F., Fadiloglu S. *Food Chemistry, Nobel Yayin Dagitim* (2006)
- [6] Alibolandi M., Hadizadeh F. et al.: Design and fabrication of an aptasensor for chloramphenicol based on energy transfer of CdTe quantum dots to graphene oxide sheet. *Mater. Sci. Eng.* 48 (2015) 611-619.
- [7] Govindasamy M. et al.: Molybdenum disulfide nanosheets coated multiwalled carbon nanotubes composite for highly sensitive determination of chloramphenicol in food samples milk, honey and powdered milk. *J Colloid Interface Sci* 485 (2017) 129-136.
- [8] Chuanuwatanakul S., Chailapakul O., Motomizu S.: Electrochemical analysis of chloramphenicol using boron-doped diamond electrode applied to a flow injection system. *Anal. Sci.* 24 (4) (2008) 493-498.
- [9] Borowiec J., Wang R., Zhu L., Zhang J.: Synthesis of nitrogen-doped graphene nanosheets decorated with gold nanoparticles as an improved sensor for electrochemical determination of chloramphenicol. *Electrochim. Acta* 99 (2013) 138-144.
- [10] Duan N., Wu S. et al.: Advances in aptasensors for the detection of food contaminants. *Analyst* 141 (2016) 3942-3961.
- [11] Wiest D.B., Cochran F., Tecklenburg F.: Chloramphenicol toxicity revisited: a 12-year-old patient with a brain abscess. *J. Pediatr. Pharmacol. Therap.* 17 (2) (2012) 182-188.
- [12] Yang G., Zhao F.: Electrochemical sensor for chloramphenicol based on novel multiwalled carbon nanotubes molecularly imprinted polymer. *Biosens. Bioelectron.* 64 (2015) 416-422.
- [13] Muller A. et al: Archimedean synthesis and magic numbers: "sizing" giant molybdenum-oxide-based molecular spheres of the keplerate type. *Angew Chem Int Ed* 38 (1999) 3238-3241.
- [14] Dutta T., Sarkar S.: Nanocarbon- $[(Na_{10}(PrW_{10}O_{36}))_2 \cdot 130H_2O]$  composite to detect toxic food coloring dyes at nanolevel. *Appl Nanosci* 6(8) (2016) 1191-1197.
- [15] Berman A., Ahn D.J., Lio A., Salmeron M.: Total alignment of calcite at acidic polydiacetylene films: cooperativity at the organic-inorganic interface. *Science* (1995) 269: 515.
- [16] Lu Y., Yang Y., Sellinger A., Lu M., Huang J., Fan H., et al.: Self-assembly of mesoscopically ordered chromatic polydiacetylene/silica nanocomposites. *Nature* 410 (2001) 913-917.
- [17] Min-Cheol Lim and Young-Rok Kim.: Analytical Applications of Nanomaterials in Monitoring Biological and Chemical Contaminants in Food. *J. Microbiol. Biotechnol.* 26(9) (2016) 1505-1516.
- [18] Reichert A., Nagy J.O., Spevak W., Charych D.: Polydiacetylene liposomes functionalized with sialic acid bind and colorimetrically detect influenza virus. *J. Am. Chem. Soc.* 117 (1995) 829-830.
- [19] Kim J.M., Lee Y.B. et al.: A polydiacetylene-based fluorescent sensor chip. *J. Am. Chem. Soc.* 127 (2005) 17580-17581.
- [20] Okada S., Peng S., Spevak W., Charych D.: Color and chromism of polydiacetylene vesicles. *Acc. Chem. Res.* 31 (1998) 229-239.
- [21] Akter H., Shaikh A.A., Chowdhury T.R. et al.: Gold nanoparticle-modified indium tin oxide electrode for highly sensitive electrochemical detection of melamine. *ECS Electrochem Lett* 2(8) (2013) 13-15.
- [22] Chen N. et al.: Determination of melamine in food contact materials using an electrode modified with gold nanoparticles and reduced graphene oxide. *Microchim Acta* 182 (2015) 1967-1975.
- [23] Yang S.P., Ding J.H., Zheng J., Hu B., Li J.Q., Chen H.W., Zhou Z.Q., Cui X.L.: Detection of melamine in milk products by surface desorption atmospheric pressure chemical ionization mass spectrometry. *Anal Chem* 81(7) (2009) 2426-2436.
- [24] Li J.H., Kuang D.Z., Feng Y.G., Zhang F.Z., Xu Z.F., Liu M.Q.: A novel electrochemical method for sensitive detection of melamine in infant formula and milk using ascorbic acid as recognition element. *Bull Kor Chem Soc* 33(8) (2012) 2499-2507.
- [25] Vasimalai N., John S.A.: Picomolar melamine enhanced the fluorescence of gold nanoparticles: spectrofluorimetric determination of melamine in milk and infant formulas using functionalized triazole capped gold nanoparticles. *Biosens Bioelectron* 42 (2013) 267-272.

## References

- [26] Wen Y.Y., Liu H.T. et al.: Determination of melamine in milk powder, milk and fish feed by capillary electrophoresis: a good alternative to HPLC. *J Sci Food Agric* 90(13) (2010) 2178-2182.
- [27] Sun H.W., Wang L.X., Ai L.F., Liang S.X., Wu H.: A sensitive and validated method for determination of melamine residue in liquid milk by reversed phase high-performance liquid chromatography with solid-phase extraction. *Food Control* 21(5) (2010) 686-691.
- [28] Xu X.M., Ren Y.P. et al.: Direct determination of melamine in dairy products by gas chromatography/mass spectrometry with coupled column separation. *Anal Chim Acta* 650(1) (2009) 39-43.
- [29] Dai H.C., Shi Y.L., Wang Y.J., et al.: Label-free turn-on fluorescent detection of melamine based on the anti-quenching ability of  $Hg^{2+}$  to gold nanoclusters. *Biosens Bioelectron* 53 (2014) 76-81.
- [30] Ai K.L., Liu Y.L., Lu L.H.: Hydrogen-bonding recognition-induced color change of gold nanoparticles for visual detection of melamine in raw milk and infant formula. *J Am Chem Soc* 131(27) (2009) 9496-9497.
- [31] Xu Q., Wei H.P., Du S., et al.: Detection of subnanomolar melamine based on electrochemical accumulation coupled with enzyme colorimetric assay. *J Agric Food Chem* 61(8) (2013) 1810-1817.
- [32] Zhang J.M., Qu S.C., Zhang L.S., et al.: Quantitative surface enhanced raman scattering detection based on the Bsandwich<sup>^</sup> structure substrate. *Spectrochim Acta A* 79(3) (2011) 625-630.
- [33] Cao Q., Zhao H., Zeng L.X., Wang J., Wang R., Qiu X.H., He Y.J.: Electrochemical determination of melamine using oligonucleotides modified gold electrodes. *Talanta* 80(2) (2009) 484-488.
- [34] Chen D., Tang L.H., Li J.H.: Graphene-based materials in electrochemistry. *Chem Soc Rev* 39(8) (2010) 3157-3180.
- [35] Li S.J., Deng D.H., Shi Q., Liu S.R.: Electrochemical synthesis of a graphene sheet and gold nanoparticle-based nanocomposite and its application to amperometric sensing of dopamine. *Microchim Acta* 177(3-4) (2012) 325-331.
- [36] Ma X.M., Liu Z.N., et al.: Simultaneous determination of hydroquinone and catechol based on glassy carbon electrode modified with gold-graphene nanocomposite. *Microchim Acta* 180(5-6) (2013) 461-468.
- [37] Soukka T., Antonen K., Harma H., et al.: Highly sensitive immunoassay of free prostate-specific antigen in serum using europium (III) nanoparticle label technology. *Clin Chim Acta* 328 (2003) 45-58.
- [38] Soukka T., Halrmal H., Paukkunen J., Lovlgren T.: Utilization of kinetically enhanced monovalent binding affinity by immunoassays based on multivalent nanoparticle-antibody bioconjugates. *Anal Chem* 73 (2001) 2254-2260.
- [39] Yang H., Li H., Jiang X.: Detection of foodborne pathogens using bioconjugated nanomaterials. *Microfluid Nanofluid* 5 (2008) 571-583.
- [40] Tan W., Wang K., He X., Zhao X.J., et al.: Bionanotechnology based on silica nanoparticles. *Med Res Rev* 24(5) (2004) 621-638.
- [41] Gu H.W., Xu K., Xu C., Xu B.: Biofunctional magnetic nanoparticles for protein separation and pathogen detection. *Chem Commun* 9 (2006) 941-949.
- [42] Lin Y.S., Tsai P.J., Weng M.F., Chen Y.C.: Affinity capture using vancomycin-bound magnetic nanoparticles for the MALDI-MS analysis of bacteria. *Anal Chem* 77(6) (2005) 1753-1760.
- [43] Basu M., Seggerson S., Henshaw J., Jiang J., et al.: Nanobiosensor development for bacterial detection during human kidney infection: use of glycoconjugate-specific antibody-bound gold NanoWire arrays (GNWA). *Glycoconj J* 21 (2004) 487-496.
- [44] Edgar R., McKinstry M., Hwang J., Oppenheim A., B., Fekete R., A., Giulian G., Merril C., Nagashima K., Adhya S.: High sensitivity bacterial detection using biotin-tagged phage and quantum-dot nanocomplexes. *Proc Natl Acad Sci USA* 103(13) (2006) 4841-4845.
- [45] El-Boubbou K., Gruden C., Huang X.: Magnetic glyconanoparticles: a unique tool for rapid pathogen detection, decontamination, and strain differentiation. *J Am Chem Soc* 129(44) (2007) 13392-13393.
- [46] Lee L.Y., Ong S.L., Hu J.Y., Ng W.J., Feng Y., Tan X., Wong S.W.: Use of semiconductor quantum dots for photostable immunofluorescence labeling of *Cryptosporidium parvum*. *Appl Environ Microbiol* 70(10) (2004) 5732-5736.
- [47] Ho J.A., Hsu H.W.: Predures for preparing *Escherichia coli* O157:H7 immunoliposome and its application in liposome immunoassay. *Anal Chem* 75 (2003) 4330-4334.
- [48] Chen C.S., Baemner A.J., Durst R.A.: Protein G-liposomal nanovesicles as universal reagents for immunoassays. *Talanta* 67 (2005) 205-211.
- [49] Chen C.S., Durst R.A.: Simultaneous detection of *Escherichia coli* O157:H7, *Salmonella* spp. and *Listeria monocytogenes* with an array-based immunosorbent assay using universal protein G-liposomal nanovesicles. *Talanta* 69 (2006) 232-238.
- [50] Wang L., Zhao W., et al.: Fluorescent nanoparticles for multiplexed bacteria monitoring. *Bioconjug Chem* 18(2) (2007) 297-301.
- [51] Tiwari S.K., Kumar V., Huczko A., Oraon R., et al.: Magical Allotropes of Carbon: Prospects and Applications, *Critical Reviews in Solid State and Materials Sciences* 41(4) (2016) 257-317.
- [52] Gambini J., Ingles M., Olaso G., Lopez-Gruoso R., et al.: Properties of resveratrol: In vitro and in vivo studies about metabolism, bioavailability, and biological effects in animal models and humans. *Oxidative Medicine and Cellular Longevity* (2015) 837042.
- [53] Huang X et al.: Resveratrol encapsulation in core-shell biopolymer nanoparticles: Impact on antioxidant and anticancer activities. *Food Hydrocolloids* 64 (2017) 157-165.
- [54] Neves A.R., Lucio M., Lima J.L.C., Reis S.: Resveratrol in medicinal chemistry: A critical review of its pharmacokinetics, drug-delivery, and membrane interactions. *Current Medicinal Chemistry* 19(11) (2012) 1663-1681.
- [55] Summerlin N., Soo E., Thakur S., Qu Z., Jambhunkar S., Popat A.: Resveratrol nanoformulations: Challenges and opportunities. *International Journal of Pharmaceutics* 479(2) (2015) 282-290.
- [56] Isailovic B.D., Kostic I.T., Zvonar A., ĐorCević V.B., et al.: Resveratrol loaded liposomes produced by different techniques. *Innovative Food Science & Emerging Technologies* 19 (2013) 181-189.
- [57] Yong Ch.W.: Study of interactions between polymer nanoparticles and cell membranes at atomistic levels. *Philosophical Transaction B* (2017)
- [58] Monteiro-Riviere N.A., Tran C.L.: *Nanotoxicology: progress toward nanomedicine*, 2<sup>nd</sup> edn. Boca Raton, FL: CRC Press. (2014)
- [59] Thake T.H.F., Webb J.R., Nash A., Rappoport J.Z., Notman R.: Permeation of polystyrene nanoparticles across model lipid bilayer membranes. *Soft Matter* 9, 10 (2013) 265-274.
- [60] Yu T.: Surfactant Assisted Dispersion of Single-Walled Carbon Nanotubes in Polyvinylpyrrolidone Solutions. *Electronic Thesis and Dissertation Repository* (2014)
- [61] O'Connell M.J. et al.: Reversible water-solubilization of single-walled carbon nanotubes by polymer wrapping. *Chem. Phys. Lett.* 342 (2001) 265-271.
- [62] Maity A., Sinha Ray S., Hato M.J.: The bulk polymerisation of N-vinylcarbazole in the presence of both multi- and single-walled carbon nanotubes: A comparative study. *Polymer* 49 (2008) 2857-2865.
- [63] Zheng M., et al.: DNA-assisted dispersion and separation of carbon nanotubes. *Nat. Mater.* 2 (2003) 338-342.
- [64] Dror Y., Pyckhout-Hintzen W., Cohen Y.: Conformation of Polymers Dispersing Single-Walled Carbon Nanotubes in Water: A Small-Angle Neutron Scattering Study. *Macromolecules* 38 (2005) 7828-7836.
- [65] Yang K., Zhu L.Z., Xing B.S.: Adsorption of polycyclic aromatic hydrocarbons by carbon nanomaterials. *Environmental Science & Technology* 40(6) (2006) 1855-1861.
- [66] Peng H.B., Pan B., et al.: Adsorption of ofloxacin and norfloxacin on carbon nanotubes: hydrophobicity- and structure-controlled process. *Journal of Hazardous Materials* 89-96 (2012) 233-234.
- [67] Tourmus F., Charlier J.C.: Ab initio study of benzene adsorption on carbon nanotubes. *Physical Review B* (2005) 71(16):165421.
- [68] Gotovac S., Song L., Kanoh H., et al.: Assembly structure control of single wall carbon nanotubes with liquid phase naphthalene adsorption. *Colloids and Surfaces A: Physicochemical and Engineering Aspects* 300(1-2) (2007) 117-121.
- [69] Yang Y.N., Chun Y., Sheng G.Y., et al.: pH-dependence of pesticide adsorption by wheat-residue-derived black carbon. *Langmuir*, 20(16) (2004) 6736-6741.
- [70] Zhang S.J., Shao T., Bekaroglu S.S.K., et al.: Adsorption of synthetic organic chemicals by carbon nanotubes: effects of background solution chemistry. *Water Research* 44(6) (2010) 2067-2074.
- [71] Hu J., Shao D.D., Chen C.L., et al.: Plasma-induced grafting of cyclodextrin onto multiwall carbon nanotube/iron oxides for adsorbent application. *The Journal of Physical Chemistry B* 114(20) (2010) 6779-6785.
- [72] Ravichandran R.: *Nanotechnology Applications in Food and Food Processing: Innovative Green Approaches, Opportunities and Uncertainties for Global Market*. *International Journal of Green Nanotechnology: Physics and Chemistry* (2010).

